frontiers | Frontiers in Earth Science

TYPE Original Research
PUBLISHED 22 June 2023
DOI 10.3389/feart.2023.1162023

OPEN ACCESS

EDITED BY
Pauline Guenser,
Université de Bordeaux, France

REVIEWED BY
Andrey Zhuravlev,
Institute of Biology, Russia
Li Tian,
China University of Geosciences Wuhan, China

*CORRESPONDENCE
Shun Muto,
s-muto@aist.go.jp
Satoshi Takahashi,
stakahashi@eps.nagoya-u.ac.jp

RECEIVED 09 February 2023
ACCEPTED 12 June 2023
PUBLISHED 22 June 2023

CITATION
Muto S, Takahashi S and Murayama M (2023), Conodont biostratigraphy of a Carboniferous–Permian boundary section in siliceous successions of pelagic Panthalassa revealed by X-ray computed microtomography. *Front. Earth Sci.* 11:1162023. doi: 10.3389/feart.2023.1162023

Conodont biostratigraphy of a Carboniferous–Permian boundary section in siliceous successions of pelagic Panthalassa revealed by X-ray computed microtomography

Shun Muto[1]*, Satoshi Takahashi[2]* and Masafumi Murayama[3,4]

[1]Geological Survey of Japan, National Institute of Advanced Industrial Science and Technology, Tsukuba, Japan, [2]Department of Earth and Environmental Sciences, Nagoya University, Nagoya, Japan, [3]Department of Marine Resource Science, Faculty of Agriculture and Marine Science, Kochi University, Nankoku, Japan, [4]Center for Advanced Marine Core Research, Kochi University, Nankoku, Japan

Pelagic deep-sea siliceous successions in accretionary complexes preserve precious records of a vast deep seafloor that is now lost due to plate subduction. Microfossils are the key means of age assignment of these successions, but poor preservation due to tectonic deformation and metamorphism at the subduction zone hamper biostratigraphic records. X-ray computed microtomography, while not widely used in biostratigraphic studies until now, allows us to visualize fossils that are impossible or difficult to extract from host rocks due to poor preservation. In this study, we applied this method on conodonts from a pelagic chert–claystone succession in Okoshizawa, Iwaizumi Town, Northeast Japan, using a laboratory-based X-ray microscope. This work is a first close look at conodont biostratigraphy across the Carboniferous–Permian boundary in pelagic deep Panthalassa. We identified conodonts including ten species that are used as zonal markers in intensely studied areas such as around the East European Platform and Midcontinent United States. Based on the occurrence of conodonts, the studied section in Okoshizawa was correlated to the lower Moscovian to middle Artinskian. Confirmation of Moscovian to Artinskian age diagnostic conodonts from pelagic Panthalassa strengthens their role as global biostratigraphic indicators. By identifying more numerous specimens compared to the conventional hydrofluoric acid dissolution method, we were able to obtain information about conodont faunal characteristics around the Carboniferous–Permian boundary in pelagic deep areas of Panthalassa. The dominant taxa changed from *Streptognathodus* to *Mesogondolella* in the middle Asselian, probably reflecting an ecological takeover by the latter in the deep waters.

KEYWORDS

accretionary complex, chert, deep-sea, North Kitakami Belt, X-ray microscope

1 Introduction

1.1 X-ray computed microtomography on microfossils from deep-sea rocks

Pelagic deep-sea siliceous successions in accretionary complexes are records of the deep seafloor that are now lost due to subduction (e.g., Isozaki et al., 1990; Wakita and Metcalfe, 2005). Due to the lack of macrofossils and datable tuff beds, microfossils are the key means of age assignment of these successions. In particular, conodonts have proved to be vital in age assignment and correlation with various Palaeozoic to Triassic marine facies in other regions (Isozaki and Matsuda, 1980; Yao et al., 1980; Yamakita et al., 2007; Hori et al., 2011; Yamashita et al., 2018; Muto et al., 2019; Tomimatsu et al., 2020). Pelagic deep-sea sections dated by conodonts are used as sedimentary records of a unique oceanic realm, which also has the advantage of covering extremely long time intervals (millions to tens of millions of years) without receiving strong local effects (Takahashi et al., 2009; Sano et al., 2010; Sano et al., 2012; Nakada et al., 2014; Takahashi et al., 2014; Muto et al., 2018; Muto et al., 2020; Tomimatsu et al., 2020; Grasby et al., 2021; Muto, 2021; Takahashi et al., 2021).

The drawback in biostratigraphic research of conodonts in pelagic deep-sea sedimentary rocks within accretionary complexes is the poor preservation of conodonts due to deformation and metamorphism at the subduction zone that hamper biostratigraphic records. Conodonts in these rocks are obtained by dissolving the host rock with dilute HF acid (introduced in Hayashi, 1968) or less commonly by observing rock pieces split parallel to the bedding plane (Yamakita et al., 1999). The former method allows extraction of conodont elements, but the yield of conodont elements is usually quite low. The latter can obtain a larger number of elements because altered and cracked specimens can be observed, but the direction of observation of the specimens is limited. In the face of these limitations, Muto et al. (2021) proposed the use of X-ray computed microtomography (X-ray μCT) as a method that offers more consistency.

X-ray computed tomography can image fossils that are buried within the host rock, and the development of X-ray microscopes and synchrotron facilities allowed application to microfossils (Ketcham and Carlson, 2001; Mees et al., 2003; Cnudde and Boone, 2013; Cunningham et al., 2014). X-ray μCT on conodonts have been introduced in recent years mainly for the purpose of morphological and palaeontological analyses, taking advantage of the high-quality 3D-morphological data and their versatility (Goudemand et al., 2011; Goudemand et al., 2012; Jones et al., 2012; Mazza and Martínez-Pérez, 2015; Martínez-Pérez et al., 2016; Zhuravlev, 2017; Guenser et al., 2019; Huang et al., 2019; Sun et al., 2020). However, the method is not widely used in biostratigraphic studies. The reason is because conodonts can be extracted relatively easily from most types of rocks containing these fossils. Hence, acquisition and rapid identification of large quantities of specimens by extraction and observation using scanning electron microscopes (SEMs) is generally the most accessible and efficient method. On the other hand, in the case of some rare types of rocks such as pelagic deep-sea siliceous rocks in accretionary complexes, X-ray μCT can be a powerful tool to visualize fossils that are not extractable using chemicals or not identifiable in limited angle of observation on rock surfaces. Zhuravlev and Gerasimova (2016) successfully used X-ray μCT to search and observe conodonts in basinal siliceous rocks. Recently, we applied X-ray μCT to siliceous rocks in accretionary

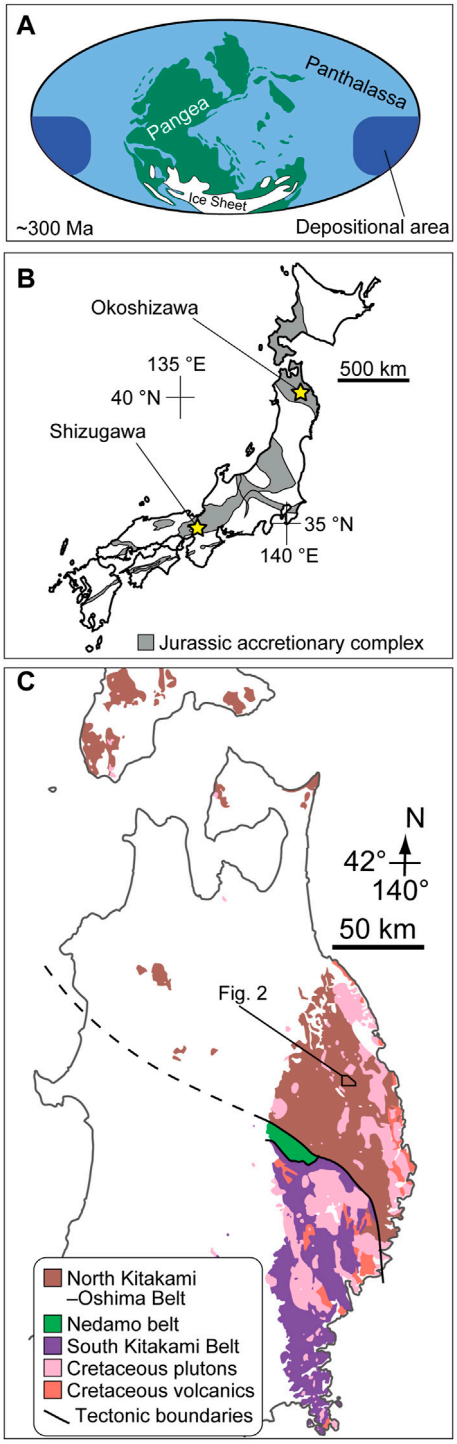

FIGURE 1
(A) Palaeogeorgaphic map by Mei and Henderson (2001) based on Ziegler et al. (1997). The depositional area of pelagic deep-sea sedimentary rocks preserved within Jurassic accretionary complexes of Japan is shown. **(B)** Distribution of the Jurassic accretionary complex in the Japanese islands in the basement rocks (based on Isozaki et al., 2010) and the location of Okoshizawa (this study; Ehiro et al., 2008) and Shizugawa (Kusunoki et al., 2004). **(C)** Exposure of pre-Paleogene rocks in northern Tohoku of Northeast Japan (modified from Geological Survey of Japan, AIST, 2020).

complexes that have undergone greater diagenesis and showed that it is in many cases the most consistent means to observe conodonts in these rocks (Muto et al., 2021).

1.2 The Carboniferous–Permian boundary

This study focuses on the Carboniferous–Permian boundary (CPB) in deep-sea sedimentary rocks deposited in pelagic Panthalassa. Conodont biostratigraphy was used for age assignment of stratigraphic intervals around the CPB in classic sections around the East European Platform centred in western Russia (Barskov et al., 1981; Chernykh and Reshetkova, 1987; Sobolev and Nakrem, 1996; Chernykh and Ritter, 1997) and Midcontinent United States (von Bitter, 1972; Perlmutter, 1975; Ritter, 1995). The Global Stratotype Section and Point (GSSP) of the CPB was ratified in Aidaralash Creek, Aktöbe, northern Kazakhstan which is situated in the marginal area of the East European Platform, and the first appearance datum of the conodont *Streptognathodus isolatus* was chosen as the definition of the boundary (Davydov et al., 1998). The conodont-based boundary definition and age correlation was adopted in other regions including South China (Wang and Qi, 2003), Japan (Kusunoki et al., 2004) and South America (Suárez-Riglos et al., 1987). Monographic studies following the ratification of the CPB both around the East European Platform (Chernykh, 2005; Chernykh, 2006) and Midcontinent United States (Boardman et al., 2009) lead to the description of various new species, many of which were considered useful in improving the temporal resolution of conodont zonal schemes. However, conodont studies were conducted rather independently in the two regions for both the Pennsylvanian (upper Carboniferous) and Cisuralian (lower Permian). Therefore, establishment of a global scheme was, and partly remains, hampered by both endemism of conodonts and taxonomic issues (Henderson, 2018; Barrick et al., 2022).

Due to the above circumstances, accumulation of data on conodont biostratigraphy from a wide range of palaeogeographic regions is required for the establishment of a globally applicable biostratigraphic framework across the CPB. Such data will provide information on which taxa can be found universally and which are endemic to a certain region or confined to particular environments. In this sense, pelagic sedimentary rocks accumulated in Panthalassa (Figure 1A) are one of the critical pieces of information. These pelagic rocks, now only found in circum-Pacific accretionary complexes (e.g., Isozaki et al., 1990), represent a unique oceanic realm of an extremely open-marine environment. Two types of rocks represent this oceanic realm: limestone deposited on seamounts and siliceous rocks deposited on abyssal plains (e.g., Isozaki et al., 1990). The latter preserves a more long-ranging record (up to 150 million years) and also represents an oceanic environment with extremely deep bathymetry, not found in sedimentary records elsewhere (e.g., Matsuda and Isozaki, 1991).

Pelagic deep-sea successions of Carboniferous to Permian age deposited in Panthalassa are found almost exclusively in accretionary complexes in Japan. Conodont occurrences across the CPB have been reported from two localities in the Jurassic accretionary complex: Shizugawa in south Kyoto (Kusunoki et al., 2004) and Okoshizawa in north Iwate (Ehiro et al., 2008) (Figure 1B). Carboniferous to Permian conodonts were also reported from deep-sea chert in the Ashio Mountains in east Japan (Hayashi et al., 1990), but these are based on erroneous identification of Permian and Triassic conodonts (Muto and Ito, 2021). The confirmation of rocks as old as the Carboniferous from the Jurassic accretionary complex was a valuable report by itself when the works in Shizugawa and Okoshizawa were published, and efforts were not concentrated on narrowing down the CPB in both localities. In addition, these studies were published before the monographic studies around the CPB in the Urals (Chernykh, 2005, 2006) and Midcontinent United States (Boardmann et al., 2009), which means that the species concepts in the previous works in Japan are not directly comparable with that adopted today. Therefore, there is a need to refine the information on conodont biostratigraphy in the CPB interval in Panthalassic pelagic deep-sea successions based on higher sampling resolution and updated taxonomic concepts. In this study, we focus on the Okoshizawa section, which is observed in outcrops from which Ehiro et al. (2008) reported Carboniferous and Permian conodonts (locality "Ref.1" therein). This is one of the fossil localities in which Muto et al. (2021) confirmed the applicability of X-ray μCT on conodonts in pelagic deep-sea siliceous rocks. By applying the method on more samples across the CPB, we establish a correlation of this boundary interval in pelagic deep-sea sections of Panthalassa with the modern biostratigraphic schemes adopted around the East European Platform, Midcontinent United States and elsewhere.

2 Geological setting

The Okoshizawa section is exposed in a roadcut along a logging road traversing the east bank of Okoshi Stream (Okoshizawa in Japanese) in the northwest part of Iwaizumi Town, Iwate Prefecture, Tohoku, Northeast Japan (40°0′14″N 141°36′17″E) (Figures 1C, 2). We studied pelagic deep-sea sedimentary rocks (mostly bedded chert) that belong to the Jurassic accretionary complex of the North Kitakami Belt (Ehiro et al., 2008). These sedimentary rocks were deposited in the Superocean Panthalassa (Figure 1A) then transported and accreted at the subduction zone along its western margin by plate motion during the Jurassic to earliest Cretaceous (Isozaki et al., 1990; Wakita and Metcalfe, 2005; Ehiro et al., 2008; Uchino and Suzuki, 2020).

The geology of the area around Okoshizawa is detailed in Ehiro et al. (2008) and Muto et al. (2023) (Figure 2). The pelagic deep-sea sedimentary rocks in Okoshizawa mostly comprise bedded chert and siliceous claystone of the Otori Unit of Takahashi et al. (2016) (revised by Muto et al., 2023). The Otori Unit is mainly composed of stacked sheets of coherent sequences of pelagic deep-sea chert and hemipelagic siliceous mudstone in the structurally lower part (Okoshizawa Subunit), and mixed rock facies in the structurally upper part (Osakamoto Subunit) (Figure 2; Muto et al., 2023). The Okoshizawa section belongs to the Okoshizawa Subunit and corresponds to the stratigraphically lowermost part of a coherent succession of chert and siliceous mudstone (Muto et al., 2023). The confirmed age of chert ranges from Pennsylvanian to Upper Triassic (Ehiro et al., 2008; Takahashi et al., 2009; Muto et al., 2021; Muto et al., 2023), and its youngest limit likely extends into the Lower Jurassic based on the Middle Jurassic age of the conformably overlying siliceous mudstone (Suzuki et al., 2007; Muto et al., 2023).

The Okoshizawa section is composed of brownish yellow dolostone with greenish grey chert interbeds, greenish grey chert,

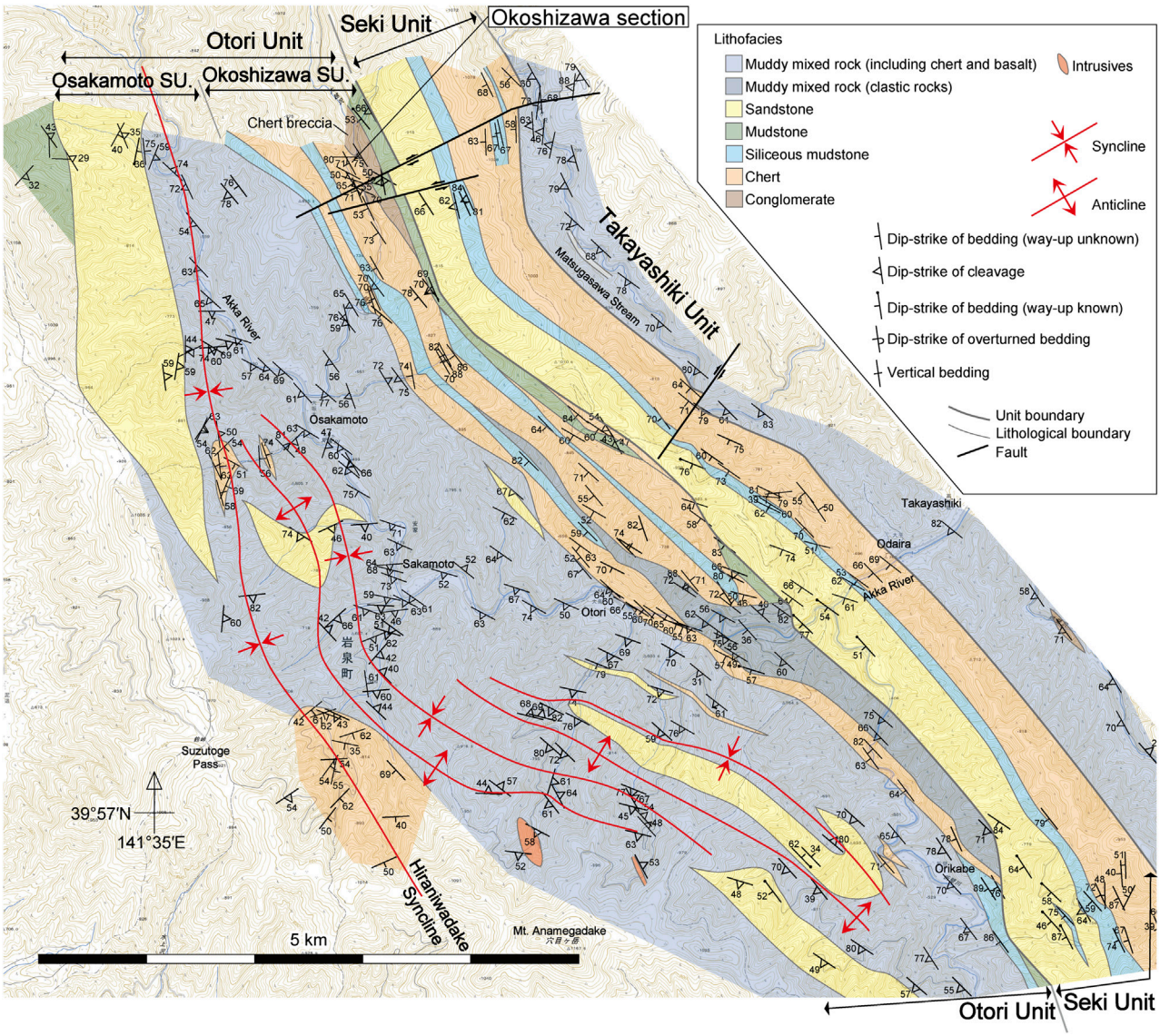

FIGURE 2
Geological map of the Akka area (Muto et al., 2023). The Okoshizawa section is situated in the Okoshizawa Subunit composed mainly of stacked sheets of coherent chert–siliceous mudstone sequences. Base map from 1: 25,000 topographic map "Akkamori", "Rikuchu-Itsukaichi", "Hashigami" and "Akka" by the Geospatial Authority of Japan. SU. Subunit.

green claystone, dark red siliceous claystone with grey and white chert interbeds and grey bedded chert in ascending order, consistent with the brief report by Ehiro et al. (2008) (Figure 3). Basaltic volcaniclastics are exposed in a separated outcrop apparently ~40 m below the base of the section, but the stratigraphic relationship between the basaltic rocks and dolostone at the base of the Okoshizawa section is unknown. The lithologies that constitute the Okoshizawa section have been described by Muto et al. (2023), and this study presents a detailed lithostratigraphy (Figure 4).

The lowermost part of the section is composed of mostly1–5 cm-thick dolostone beds with 1–10 cm-thick greenish grey chert interbeds with a total thickness of ~2 m. The thickest dolostone bed is 40 cm thick. Overlying this is greenish grey chert, separated by a covered area from the underlying strata. It is approximately 1.6 m thick and is well-bedded with single bed thickness of generally 2–5 cm. Green siliceous claystone is in contact with the greenish grey chert with a fault and has a total thickness of approximately 1 m. It is somewhat weakly bedded (i.e., the bedding plane is not laterally traceable in some cases) with single bed thickness of generally 2–5 cm. Greyish cherty layers are present within the green siliceous claystone, although not conspicuous at the outcrop surface. Dark red siliceous claystone conformably overlies the green siliceous claystone and attains approximately 10.3 m in total thickness. There are three bedding parallel slip planes of which one diminishes within the observed area of the outcrop, whereas two ("fault?" in Figures 3C,D) extend further and may cause gaps in the lithostratigraphy. One of the bedding parallel slip planes are accompanied by an isoclinal fold pair. The red siliceous claystone is also somewhat weakly bedded with single bed thickness of generally 2–5 cm. White chert layers, often laterally

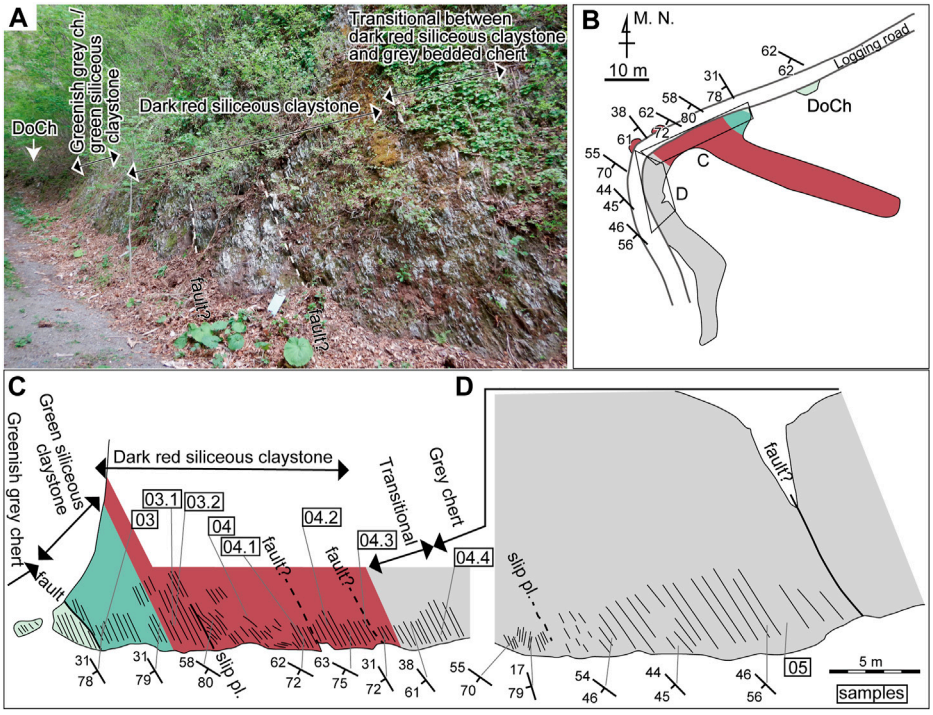

FIGURE 3
(A) Photograph of the roadcut where the Okoshizawa section is exposed. DoCh: outcrop of dolostone with greenish grey chert interbeds. The blue board in the centre is 20 cm × 30 cm. The fault and slip plane in the left side of **(C)** is not shown in here. **(B)** Sketch of the outcrops of the Okoshizawa section in plan view. See **(C)** for legends for colour. **(C, D)** Sketch of the outcrop of the main part of the Okoshizawa section. Sampled horizons are indicated by sample IDs ("Okz-CO-" is abbreviated) enclosed in rectangles.

discontinuous and nodule-like, occur within the red siliceous claystone. The lithofacies changes upsection to grey bedded chert with a transitional zone approximately 2.2 m thick. The grey chert is 8 m thick measured to the fault at the top of the logged interval and is well-bedded with single bed thickness of mostly 3–10 cm. There is an isoclinal fold pair in the lower part, above which a bedding-parallel slip plane occurs (Figure 3D). Grey bedded chert south of the fault that marks top of the section (Figure 3D) is not logged in detail in this study. The presence of dolomite accompanied by minor basaltic fragments in the lowermost part (Muto et al., 2023) implies inputs from topographic highs such as oceanic islands, whereas the total lack of silt-size or larger detrital grains indicate deposition in a remotely pelagic setting.

Ehiro et al. (2008) previously reported *Mesogondolella clarki*, *Gondolella gymna*, *Idiognathodus delicatus*, *Idiognathoides sinuatus*, *Diplognathodus atetsuensis* and *Diplognathodus coloradoensis* from the greenish grey chert intercalated in dolostone, and *Streptognathodus elongatus*, *Gondolella* cf. *bella* sensu Clark and Mosher (1966), *Mesogondolella bisselli* and *Sweetognathus* cf. *whitei* from the red siliceous claystone (their "tuffaceous chert"), but with no illustrations. Muto et al. (2021) used X-ray μCT on specimens on rock pieces and identified *St. elongatus* and *Streptognathodus bellus*. These conodonts indicate a Moscovian to Artinskian (middle late Carboniferous to middle early Permian) age. However, *M. bisselli* and *Sw. whitei* are now considered to have ranges that do not overlap (e.g., Henderson, 2018; Petryshen et al., 2020). The apparent discrepancy with the occurrence of conodonts reported by Ehiro et al. (2008) may be due to taxonomic issues or because the two species were obtained from different levels in the red siliceous claystone. The absence of lithostratigraphic columns in Ehiro et al. (2008) precludes further discussions on the age of the section including the exact position of the CPB.

3 Methods

Methods to obtain conodont specimens from deep-sea siliceous rocks and perform X-ray μCT scanning is described in detail in Muto et al. (2021). The following is a brief summary. Conodont elements were found by observing cleaved rock pieces under a stereoscopic microscope (Muto et al., 2019). Rock pieces containing well-preserved specimens were selected and trimmed down to blocks of a few millimetres. The specimens on the rock pieces were enclosed in a "hedge" of concrete mortar to avoid effects of surface refraction in the CT images, glued onto the end of a pencil lead and scanned using a ZEISS Xradia 410 versa X-ray microscope equipped with a L8121-03 SEL X-ray source of Hamamatsu Photonics K.K. at the Center for Marine Core Research, Kochi University. Scans for imaging of conodont elements were conducted with spatial resolutions of 1 μm^3/voxel, 1.5 μm^3/voxel or 2 μm^3/voxel depending on the size of the specimens (see Supplementary Table S1 for details). Three-dimensional images of the fossils were produced by Amira Software (Thermo Fisher Scientific).

We also performed the conventional extraction method of conodonts using dilute hydrofluoric (HF) acid; 16 cycles (8 or 16 h per cycle) using 5–10wt% HF acid (following the method of

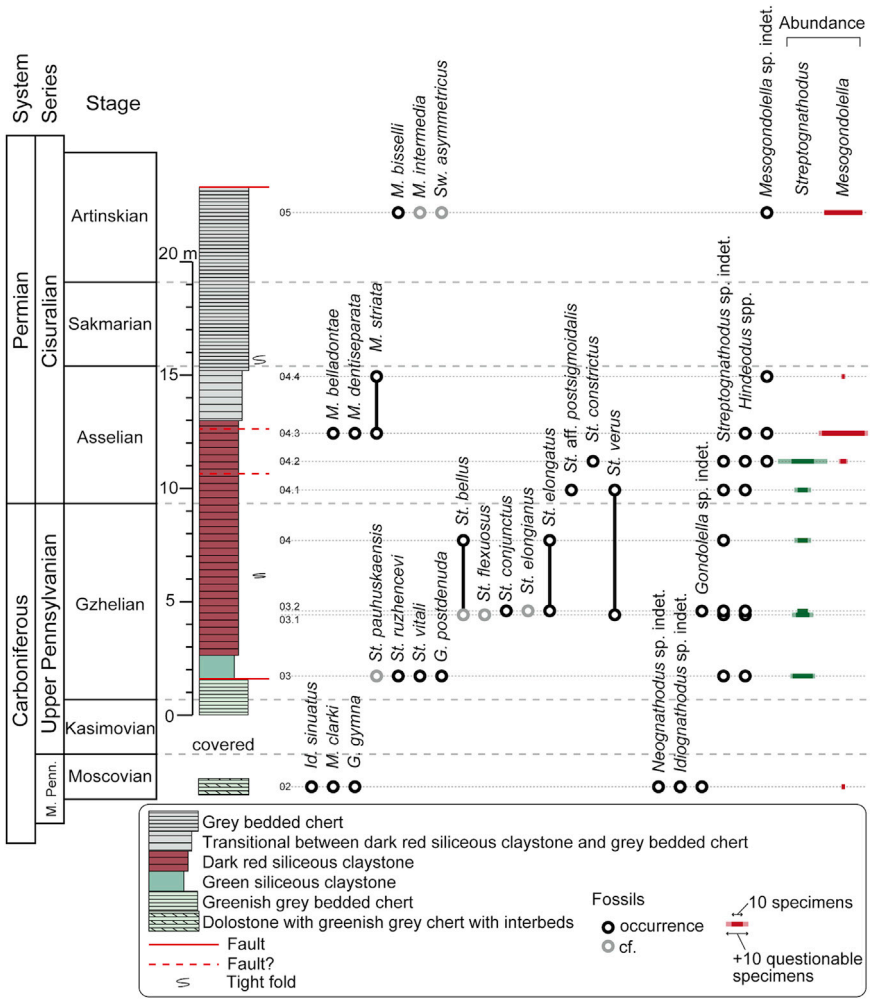

FIGURE 4
Lithostratigraphic column and conodont occurrence of the Okoshizawa section. Sample Okz-CO-04 was studied in Muto et al. (2021). M. Penn. Middle Pennsylvanian; *Id. Idiognathoides*; *M. Mesogondolella*; *G. Gondolella*; *St. Streptognathodus*; *Sw. Sweetognathus*. The prefix "Okz-CO-" is abbreviated from sample IDs. Absolute abundance of *Streptognathodus* and *Mesogondolella* is represented by the width of horizontal bars on the far right. See Supplementary Table S2 for more details on conodont occurrence. Note that the vertical position of stage boundaries on the leftmost column is not showing their precise level in the lithostratigraphic column and uncertainties exist between samples horizons.

Nishikane et al., 2011). Greenish grey chert and green siliceous claystone yielded a number of conodont elements, but these were mostly broken fragments. Red siliceous claystone and grey chert yielded no elements. Conodonts extracted by dilute HF acid were mounted on carbon tapes and photographed by a scanning electron microscope (SEM; Hitachi SU3500) at the Geological Survey of Japan. In addition, some "clean" moulds (see results section for detail) were photographed using SEM.

4 Results

4.1 Occurrence and preservation of the conodont fossils

Conodonts in the studied section were black coloured in the greenish grey chert intercalated in dolostone and the lower part of the grey chert, dark grey in the green siliceous claystone, white to orange in the red siliceous claystone and moulds in the upper part of the grey chert (Figure 5). Of these, the black and dark grey fossils were dense material with high CT values, while the white and orange fossils were composed of material with high CT values but were less dense, probably due to recrystallization, in accordance with Muto et al. (2021). Due to this, the surface of white and orange fossils was less sharply recognized and had greater noise compared with the black and dark grey varieties. "Clean" moulds with no secondary precipitate inside were easily recognized from the host rock. When secondary precipitate was present, which was the case in many of the moulds, the surface of the fossil specimens produced from X-ray μCT was somewhat noisy. Despite some difficulties, images produced from X-ray μCT were adequate to identify many of the specimens to the species level and most to the genus level (Figures 6–8). In general, idiognathodontids were more difficult to identify compared to gondolellids because species distinctions are based on morphological features of smaller sizes.

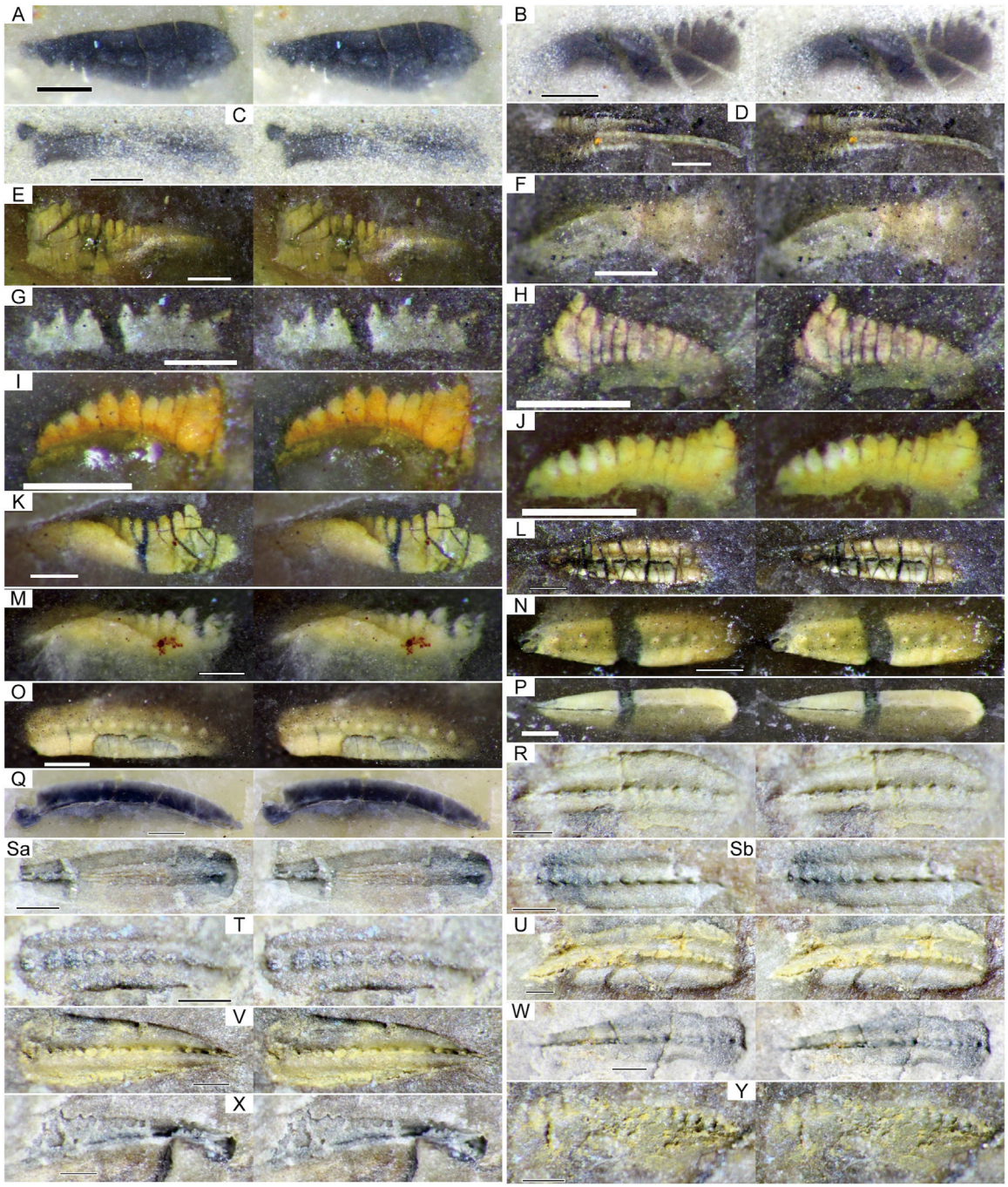

FIGURE 5
Stereographic photographs of conodonts obtained from the Okoshizawa section (parallel viewing). Note that most specimens were identified based on X-ray μCT scans (Figures 6–8) and SEM photography (Figure 9). **(A)** *M. clarki*, Okz-CO-02. **(B)** *St. vitali*, Okz-CO-03. **(C)** *G. postdenuda*, Okz-CO-03. **(D)** *St.* cf. *bellus*, Okz-CO-03.1. **(E)** *St.* cf. *flexuosus*, Okz-CO-03.1. **(F)** *St. conjunctus*, Okz-CO-03.2. **(G)** *Gondolella* sp. indet., Okz-CO-03.2. **(H)** *H. minutus*, Okz-CO-03.2. **(I, J)** *H. minutus*, Okz-CO-04.1. **(K)** *St.* aff. *postsigmoidalis*, Okz-CO-04.1. **(L)** *Mesogondolella* sp. indet., Okz-CO-04.2. **(M)** *St. constrictus*, Okz-CO-04.2. **(N, P)** *M. dentiseparata*, Okz-CO-04.3. **(O)** *M. dentiseparata* transitional to *M. striata*. **(Q)** *M. striata*, Okz-CO-04.4. **(R–T)** *M.* cf. *bisselli*, Okz-CO-05, (Sa) and (Sb) are counterparts. **(U–X)** *M.* cf. *intermedia*, Okz-CO-05. **(Y)** *Sw.* cf. *asymmetricus*. *H.*: *Hindeodus*. See Figure 4 for abbreviation of other genera. Scale bars are 200 μm.

Of the investigated samples, greenish grey chert and green siliceous claystone which contained black and dark grey conodont fossils also yielded conodont elements by dilute HF acid treatment. Samples with white and orange fossils were completely unproductive after 16 cycles of HF acid treatment. We did not perform HF acid treatment for sample Okz-CO-05,

10.3389/feart.2023.1162023

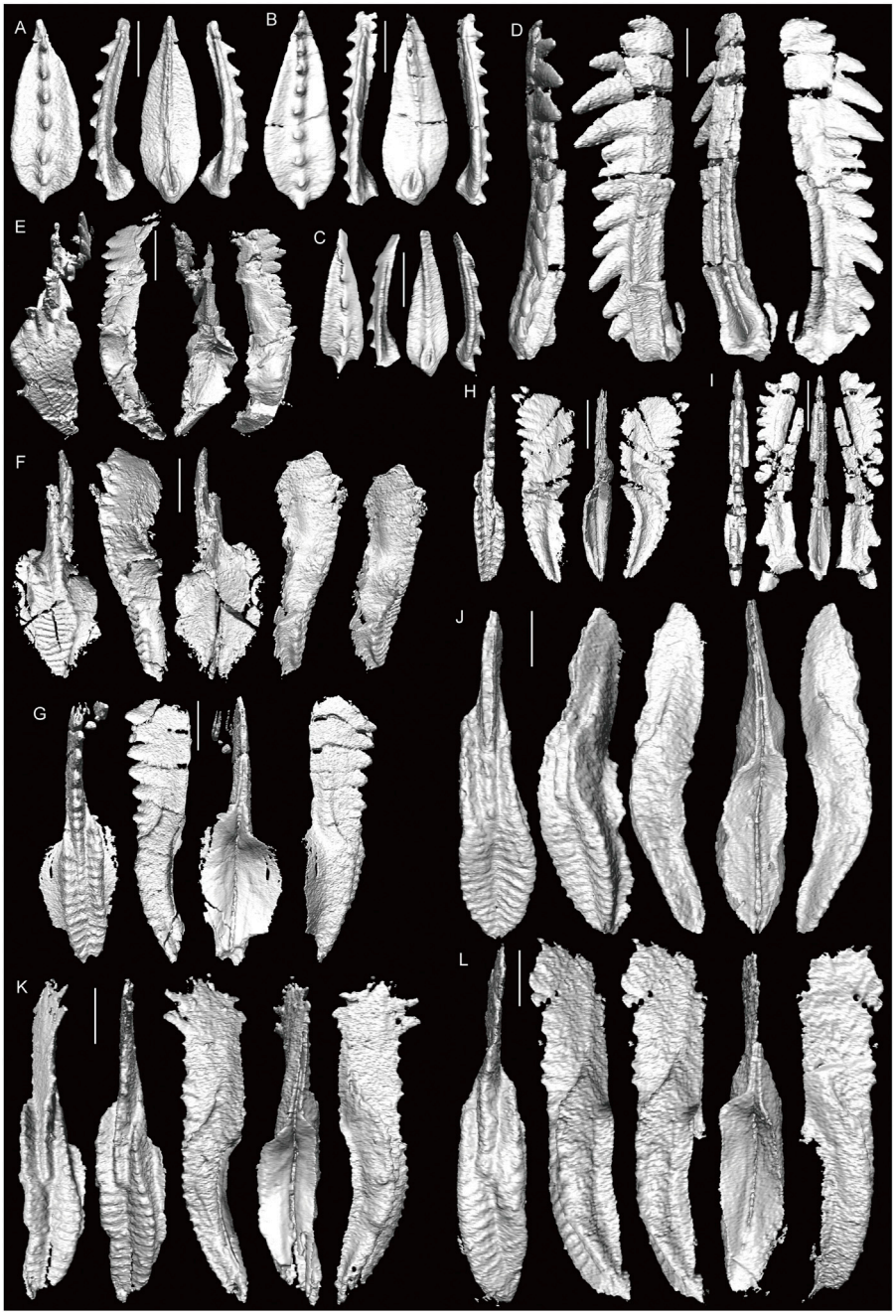

FIGURE 6
3D-images of conodonts obtained by X-ray μCT (part one). **(A–C)** *M. clarki*, Okz-CO-02; **(B)** shown in Figure 5A. **(D)** *G. gymna*, Okz-CO-02. **(E)** *Idiognathodus* sp. indet., Okz-CO-02. **(F)** *Id. sinuatus*, Okz-CO-02 **(G, H)** *St. vitali*, Okz-CO-03; **(H)** shown in Figure 5B. **(I)** *G. postdenuda*, Okz-CO-03; shown in Figure 5C. **(J, K)** *St.* cf. *bellus*, Okz-CO-03.1; **(J)** shown in Figure 5D. **(L)** *St.* cf. *flexuosus*; shown in Figure 5E. Scale bars are 200 μm.

in which conodonts were preserved as moulds. As stressed in Muto et al. (2021), the results indicate that X-ray μCT is the most consistent method of observing conodonts in the deep-sea siliceous rocks, because it enables us to observe altered specimens and cracked specimens. Altered specimens that are white or orange coloured and specimens preserved as moulds can only be observed by this method. In the case of grey or black specimens that have suffered minimal alteration, extraction by dilute HF acid is possible, but the number of identifiable conodonts obtained in the same time period is inferior compared to the method using X-ray μCT, probably because the majority of these conodonts are cracked. Indeed, most of the conodonts extracted using dilute HF acid in this study were unidentifiable fragments. In the case of the present study, X-ray μCT was absolutely crucial, because the state of preservation of conodonts in most of the investigated samples did not allow extraction using dilute HF acid.

We also performed SEM photography on some specimens preserved as "clean" moulds (Figures 9I–L). SEM photography was

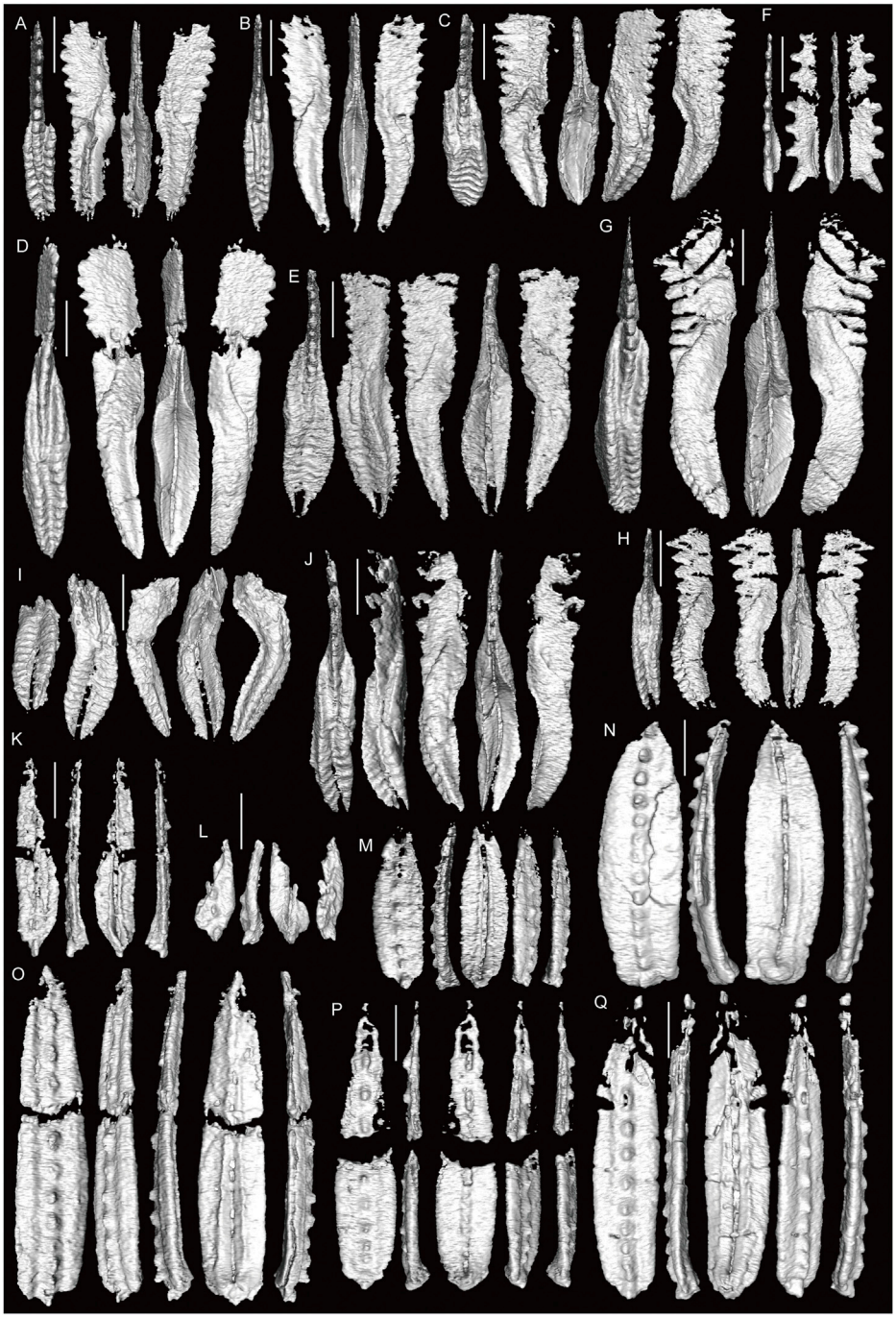

FIGURE 7
3D-images of conodonts obtained by X-ray μCT (part two). **(A)** *St. verus*, Okz-CO-03.1. **(B)** *St.* cf. *elongianus*, Okz-CO-03.2. **(C)** *St. conjunctus*, Okz-CO-03.2, shown in Figure 5F. **(D)** *St. elongatus*, Okz-CO-03.2. **(E)** *St. bellus*? Okz-CO-03.2. **(F)** *Gondolella* sp. indet., Okz-CO-03.2; shown in Figure 5G. **(G)** *St.* aff. *postsigmoidalis*, Okz-CO-04.1; shown in Figure 5K **(H)** *St. verus*, Okz-CO-04.1 **(I, J)** *St. constrictus*, Okz-CO-04.2; **(J)** shown in Figure 5M **(K, L)** *Mesogondolella* sp. indet., Okz-CO-04.2; **(K)** shown in Figure 5L. **(M, O–Q)** *M. dentiseparata*, Okz-CO-04.3; (O) shown in Figure 5P; **(P)** shown in Figure 5N. **(N)** *M. dentiseparata* transitional to *M. striata*; shown in Figure 5O. Scale bars are 200 μm.

not as effective as when performed on extracted conodonts. Compared with images based on X-ray μCT, the latter is more useful in allowing unlimited direction of observation. On the other hand, SEM has higher special resolution allowing observation of more subtle features. Sample preparation is also easier for SEM photography, in which the rock pieces need not be trimmed down to millimetre-size. However, taking SEM photographs usually requires some degree of trimming as well, and cannot be recommended for very fragile specimens. To sum up, SEM photography of moulds may be preferred over X-ray μCT when the moulds are "clean" (no precipitate on the mould walls that obscure surface topography), when trimming down the sample down to millimetre-size causes risks

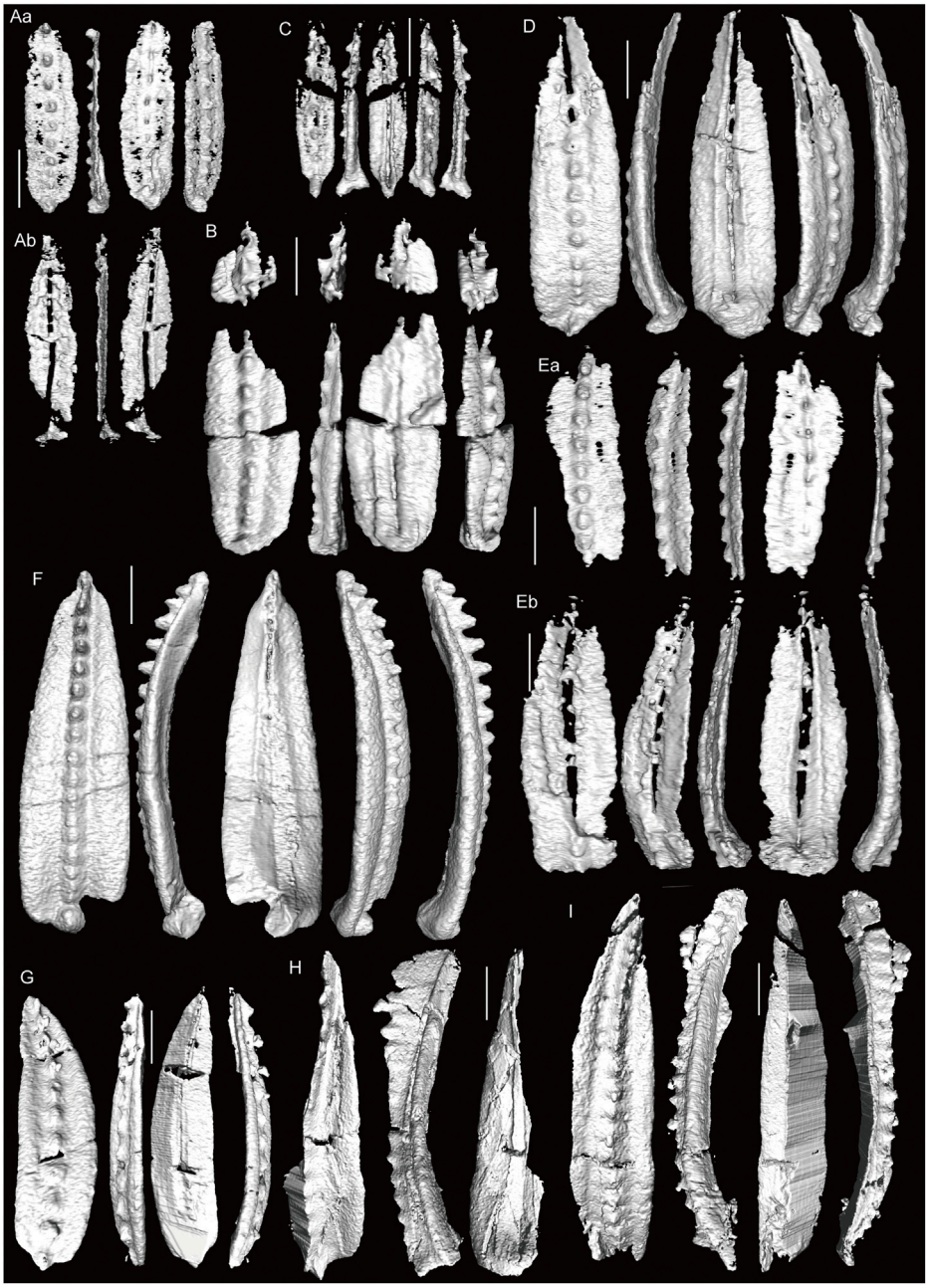

FIGURE 8
3D-images of conodonts obtained by X-ray μCT (part three). **(A, B)** *M. dentiseparata*, Okz-CO-04.3; (Aa) and (Ab) are counterparts of an element split in half. **(C, D)** *M. belladontae*, Okz-CO-04.3. **(E)** *M. striata*, Okz-CO-04.3; (Ea) and (Eb) are counterparts of an element split in half. **(F)** *M. striata*, Okz-CO-04.4; shown in Figure 5Q. **(G)** *M. bisselli*, Okz-CO-05. **(H)** *M.* cf. *intermedia*, Okz-CO-05, shown in Figure 5X. **(I)** *M. intermedia*? Okz-CO-05. Scale bars are 200 μm.

of breaking it or when the targeted morphological feature is too subtle to be obtained by X-ray μCT.

4.2 Conodont biostratigraphy of the okoshizawa section

We identified 22 conodont species belonging to six genera from a total of ten samples (Figure 4; Supplementary Table S2). In this section, the occurrence of conodonts in the Okoshizawa section is described in ascending order. The age assignment of the section is discussed in the next chapter.

Sample Okz-CO-02 which is from a greenish grey chert bed intercalated in dolostone yielded a number of segminiplanate gondolellids and carminiscaphate idiognathodontids. Gondolellid elements with a lanceolate platform outline, low, discrete denticles and a terminally located cusp with a base that creates a protrusion beyond the dorsal side of the platform were identified as *Mesogondolella clarki* (Koike) (Figures 6A–C). A gondolellid element with a blade of sharp denticles fused at the base, a

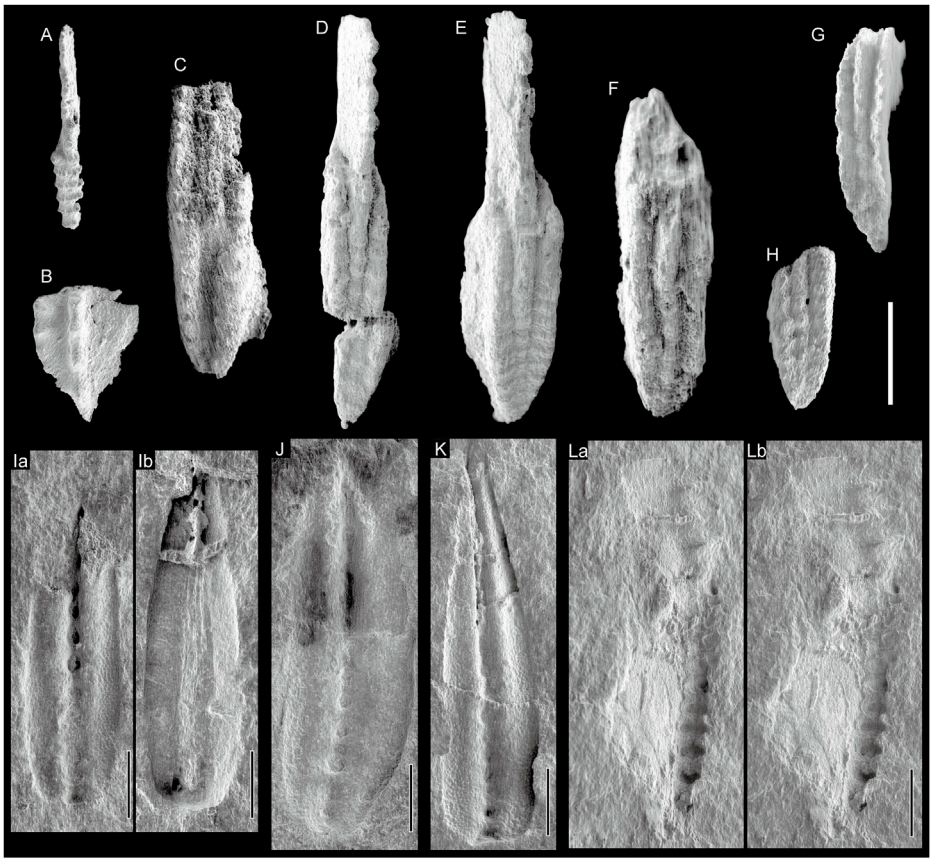

FIGURE 9
SEM photographs of conodonts obtained using dilute HF acid **(A–H)** and conodonts preserved as "clean" moulds **(I–L)** **(A)** *Idiognathoides* sp. indet., Okz-CO-02; juvenile specimen. **(B)** *Neognathodus* sp. indet., Okz-CO-02 **(C)** *St.* cf. *pauhuskaensis*, Okz-CO-04.3. **(D)** *St. ruzhencevi*, Okz-CO-03 **(D)** *St. vitali*, Okz-CO-03. **(F–H)** *St. ruzhencevi*? Okz-CO-03 **(I, J)** *M.* cf. *bisselli*, Okz-CO-05; **(Ia, Ib)** are counterparts; **(I)** shown in Figure 5S; **(J)** shown in Figure 5R **(K)** *M.* cf. *intermedia*, Okz-CO-05; shown in Figure 5W **(L)** *Sw.* cf. *asymmetricus*, Okz-CO-05; shown in Figure 5Y; (La) and (Lb) are parallel viewing stereographic pairs.

narrow platform, a wide basal cavity and a cusp broken at its thick base was identified as *Gondolella gymna* Merril and King (Figure 6D). An asymmetric carminiscaphate element with a platform crossed by uninterrupted transverse ridges that joins the blade on one side and declines into an adcarinal parapet on the other was identified as a dextral element of *Idiognathoides sinuatus* Harris and Hollingsworth (single element form species *Idiognathoides corrugatus* (Harris and Hollingsworth)) (Figure 6F). An idiognathodontid lacking a trough on the platform was identified as *Idiognathodus* sp. (Figure 6E). A juvenile element of *Idiognathoides* and a fragmented element of *Neognathodus* were extracted by treatment with dilute HF acid (Figures 9A,B). The former is distinguished by an asymmetric carminiscaphate form with the blade connecting on one lateral side of a platform covered by transverse ridges. The latter is distinguished by the carina that reaches the end of a platform with asymmetrically elevated and ornamented parapets.

Samples from the green siliceous claystone and the red siliceous claystone excluding the uppermost part (samples Okz-CO-03.1, -03.2, -04.1 and -04.2) were characterized by the dominance of carminiscaphate idiognathodontids (Figure 4). All specimens of idiognathodontids identified to the genus level belong to *Streptognathodus*, which possesses a platform with a longitudinal trough in the medial position and a carina and blade standing between adcarinal parapets.

From sample Okz-CO-03 in the green siliceous claystone, a segminiplanate gondolellid and several *Streptognathodus* elements were identified by X-ray μCT. A gondolellid element with a blade of fused stubby denticles, a moderately large terminal cusp, a narrow platform and wide basal cavity was identified as *Gondolella postdenuda* von Bitter and Merril (Figure 6I). Carminiscaphate elements with a blade that passes into a carina of nodes extending more than half the platform and short transverse ridges interrupted by a median groove was identified as *Streptognathodus vitali* Chernykh (Figures 6G,H). In addition, some *Streptognathodus* elements were extracted by dilute HF acid. Of these, one is *St. vitali*, while two others were identified as *Streptognathodus ruzhencevi* (Kozur) and *Streptognathodus* cf. *pawhuskaensis* (Harris and Hollingsworth) (Figures 9C–H). The former is distinguished by a symmetric narrow platform with carinal nodes extending to the dorsal end, and the latter by a wide and U-shaped (flat-based) median groove.

Streptognathodus from Sample Okz-CO-03.1 from the lower part of the red siliceous claystone that possess a shallow V-shaped

median groove is comparable to *Streptognathodus bellus* Chernykh and Ritter (Figures 6J,K). One of these specimens is broken on the rostral side (Figure 6K), but the 3D image is not resolved enough to show the broken part as a sharp structure. *Streptognathodus bellus* was also reported from the middle part of the red siliceous claystone (sample Okz-CO-04) by Muto et al. (2021). Sample Okz-CO-03.1 yielded two other *Streptognathodus* species. An asymmetric *Streptognathodus* element with a platform oral surface that declines more steeply in the caudal side in the dorsal portion and the median groove bending towards the caudal side is comparable to *Streptognathodus flexuosus* Chernykh and Ritter (Figure 6L). A *Streptognathodus* element with a narrow platform that has a concave caudal margin and is widest in the ventral portion was identified as *Streptognathodus verus* Chernykh (Figure 7A). This form was found again in the middle part of the red siliceous claystone (sample Okz-CO-04.1; Figure 7H). Sample Okz-CO-03.2 contained three *Streptognathodus* species. A narrow *Streptognathodus* with an irregular median groove was identified as *Streptognathodus* cf. *elongianus* Boardman et al. (Figure 7B). A narrow *Streptognathodus* with a deep median groove and moderately long carina was identified as *Streptognathodus elongatus* Gunnell (Figure 7D). A *Streptognathodus* element with a platform covered by transverse ridges that are continuous across the median groove is comparable to *Streptognathodus conjunctus* Reshetkova and Chernykh (Figure 7C). Of these, *St. elongatus* was reported from the middle part of the red siliceous claystone (sample Okz-CO-04) by Muto et al. (2021). In addition, sample Okz-CO-03.2 contained a segminate element with low discrete denticles and a wide basal cavity identified as *Gondolella* sp. (Figure 7F). Sample Okz-CO-04.1 in the upper part of the red siliceous claystone yielded a *Streptognathodus* element with a blade and carina slightly offset from the median groove that was identified as *Streptognathodus* aff. *postsigmoidalis* Chernykh (Figure 7G). Approximately 1.2 m higher (sample Okz-CO-04.2), a narrow *Streptognathodus* with a constriction of the platform around the termination of the carina was found. This form was identified as *Streptognathodus constrictus* Reshetkova and Chernykh (Figures 7I,J). In addition, this sample yielded segminiplanate elements with low discrete denticles, a small basal cavity and terminal cusp, which we place in *Mesogondolella* (Figures 7K,L).

The uppermost part of the red siliceous claystone and overlying grey bedded chert (samples Okz-CO-04.3, -04.4, -05) were dominated by segminiplanate P1 elements of *Mesogondolella* (Figure 4). The uppermost part of the red siliceous claystone (sample Okz-CO-04.3) yielded three species. Narrow *Mesogondolella* elements with a small cusp and low node-like denticles that are widely spaced particularly in the ventral portion were identified as *Mesogondolella dentiseparata* (Reshetkova and Chernykh) (Figures 7M–Q; Figure 8A). Segminiplanate elements with low widely spaced denticles and a cusp outstandingly thicker and taller than the preceding denticles were identified as *Mesogondolella belladontae* (Chernykh) (Figures 8C,D). Segminiplanate elements with low discrete denticles and a cusp that is distinguishable but not dominant were identified as *Mesogondolella striata* (Chernykh and Reshetkova) (Figure 8E). The last species also occurred from the lower part of the grey bedded chert (sample Okz-CO-04.4) (Figure 8F). A higher horizon of the grey bedded chert (sample Okz-CO-05) yielded different forms of *Mesogondolella*. Forms with low generally node-like denticles and platform margins that are sub-parallel in the middle portion, tapers in the ventral area and rounded in the dorsal margin were identified as *Mesogondolella bisselli* (Clark and Behnken) (Figure 8G) and *M.* cf. *bisselli* (Figures 5R–T; Figures 9I, J). Forms with denticles that form a fused blade in the ventral portion, a cusp that is distinguishable from the preceding denticles in thickness and height and a rounded square dorsal platform margin are comparable to *Mesogondolella intermedia* (Igo) (Figures 5V–X, 8H, 9K). In addition, this sample yielded a carminiscaphate element with a ventral blade and dorsal dome-like platform with carinal nodes that are connected by a narrow medial ridge, which was identified as *Sweetognathus* cf. *asymmetricus* Sun and Lai (*sensu* Petryshen et al., 2020) (Figures 5Y, 9L).

Carminiscaphate P1 elements of *Hindeodus* were found throughout the red siliceous claystone. Some of these specimens are identifiable as *H. minutus* (Ellison) referring to the detailed morphological study of this species by Merril (1973) (Figures 5H–J). Unfortunately, all specimens of *Hindeodus* were very poorly preserved and, although the fossils were vaguely distinguishable in individual tomographic sections from the X-ray μCT scans, it was impossible to produce accurate 3D images. This is probably due to the small size and thin nature of the *Hindeodus* elements that made them susceptible to damage by alteration.

5 Discussion

5.1 Age correlation

Classic studies on conodont biostratigraphy around the CPB were conducted around the East European Platform that includes the GSSP (e.g., Barskov et al., 1981; Akhmetshina et al., 1984; Chernykh and Retshekova, 1987; Davydov et al., 1994) and Midcontinent United States (e.g., Ritter, 1995). Detailed works on conodont biostratigraphy of intervals including the CPB have also been published from South China (e.g., Wang and Qi, 2003), western United States (Lucas et al., 2017; Ritter., 2020; Beauchamp et al., 2022b) and Arctic Canada (Beauchamp et al., 2022a). Below, we compare the occurrence of conodonts mainly with these regions to assign the age of the Okoshizawa section. Because the basal part of the Okoshizawa section yielded distinctly older conodonts compared to the rest, the basal part (sample Okz-CO-02) and the main part (all other samples) are discussed separately.

The combination of all three species from the lowermost part of the Okoshizawa section (Okz-CO-02) is not reported from other regions. Of these, *Id. sinuatus* is the most widely recognized species, occurring from around the East European Platform, central and western United States, South China (references below), Europe (Nemyrovskaya et al., 2011), Japan (Takahashi et al., 2020) and South America (Nascimento et al., 2005; Cardoso et al., 2017). It occurs in the Bashkirian to lower Moscovian in the Donets Basin (Nemyrovskaya, 1999; Nemyrovskaya et al., 1999; Fohrer et al., 2007) and the Bashkirian Mountains (Nemirovskaya and Alekseev, 1994) around the East European Platform and South China (Wang and Qi, 2003; Qi et al., 2014, 2016; Hu et al., 2017). In the United States, the range of this species ends lower, covering most

of the Morrowan regional stage, which correlates with most of the Bashkirian (Dunn, 1970; Lane and Straka, 1974; Baesemann and Lane, 1985). *Mesogondolella clarki* occurs from the upper Moscovian in the Donets Basin (Nemyrovskaya, 2011; Nemyrovskaya, 2017) and lower to middle Moscovian in South China (Wang and Qi, 2003; Qi et al., 2014; Qi et al., 2016; Hu et al., 2017). Thus, *Id. sinuatus* disappears before the appearance of *M. clarki* in the Donets Basin, while it cooccurs with *M. clarki* in the lower Moscovian in South China. *Mesogondolella clarki* is also reported from strata correlated to the upper Bashkirian and middle Moscovian in Alaska (Savage and Barkeley, 1985), but the stratigraphic distribution of conodont species used as age indicators therein appears to contradict with more intensely studied regions, suggesting that the biostratigraphy may require reconsideration. *Gondolella gymna* is recorded from the Seville limestone in Illiois (Merril and King, 1971; von Bitter and Merril, 1980), which is correlated to the middle Moscovian (Barrick et al., 2022). This species is not documented around the East European Platform or South China, although a similar form of *Gondolella* with a reduced platform and a large cusp is reported in the upper Bashkirian to lower Moscovian in the latter (Qi et al., 2016). The three species from Okoshizawa occur from seamount limestones in the Permian accretionary complex of the Akiyoshi Belt in Japan, which were also deposited in pelagic Panthalassa (Atetsu limestone, Koike, 1967; Ko-yama limestone, Ishida et al., 2013; Omi limestone, Takahashi et al., 2020). *Idiognathoides sinuatus* is only known from the Bashikirian of the Atetsu limestone, *M. clarki* is reported from the lower Moscovian in all three studied areas, and *G. gymna* is only known from the upper Bashkirian to lower Moscovian of the Omi limestone (*Gondolella*? sp. A of Koike, 1967).

Putting an emphasis on conodont occurrences around the East European Platform, Midcontinent United States and South China, it is most parsimonious to correlate the basal part of the Okoshizawa section to the lower Moscovian (Supplementary Figure S1, Supplementary Datasheet 3). This age assignment assumes that in Okoshizawa the range of *Id. sinuatus* is similar to that in South China, the Donets Basin and Bashkirian Mountains, that of *M. clarki* is similar to that in South China and that of *G. gymna* is similar to Midcontinent United States. On the other hand, the range of *M. clarki* extends lower than the Donets Basin and the range of *Id. sinuatus* extends higher than the United States in Okoshizawa.

In strata of Late Pennsylvanian age, species of *Idiognathodus* and *Streptognathodus* are used to define conodont biozones both around the East European Platform typified by sections in the Ural region (Chernykh and Ritter, 1997; Chernykh, 2005; Chernykh, 2006; Goreva and Alekseev, 2010) and in Midcontinent United States (Ritter, 1995; Barrick et al., 2004; Barrick et al., 2013; Barrick et al., 2022). In the lower Cisuralian, species of *Streptognathodus*, *Sweetognathus* and *Mesogondolella* are considered as key age indicators in the Ural region (Chernykh, 2005, 2006), while the former two genera are mainly used in Midcontinent United States (Boardman et al., 2009). *Steptognathodus*-based zones of the Upper Pennsylvanian to lowermost Cisuralian have been reproduced in South China (Wang and Qi, 2003; Hu et al., 2020). A number of stratigraphically important species of *Streptognathodus* have been confirmed as widely distributed, including *Streptognathodus isolatus*, which defines the CPB (Davydov et al., 1998). Earliest Permian species of *Mesogondolella* were originally known only from the Ural region (Chernykh and Reshetkova, 1987; Chernykh, 2005; Chernykh, 2006), but have recently been found from Nevada (Wardlaw et al., 2015; Beauchamp et al., 2022b) and the Sverdrup Basin (Beauchamp et al., 2022a), confirming the validity of this group as correlation markers.

Streptognathodus vitali from sample Okz-CO-03 in the green siliceous claystone of the Okoshizawa section is a zonal marker species for the lower Gzhelian both around the East European Platform (Chernykh, 2005, 2006; Goreva and Alekseev, 2010) and in Midcontinent United States (Barrick et al., 2013; Barrick et al., 2022). This species also occurs in the lower Gzhelian of South China (Hu et al., 2020). *Streptognathodus pauhuskaensis* and *St. ruzhencevi* are species that respectively have lowest occurrences (LOs) below and above that of *St. vitali*, and cooccur in the lower Gzhelian *St. vitali* Zone around the East European Platform (Goreva and Alekseev, 2010) and in Midcontinent United States (Barrick et al., 2013; Barrick et al., 2022). In South China, *St. pauhuskaensis* occurs from the upper Kasimovian to lower Gzhelian (Wang and Qi, 2003; Hu et al., 2020). The sample from Okoshizawa also yielded *G. postdenuda*, a species that occurs from the lower Gzhelian with *St. vitali* (von Bitter and Merril, 1980; Heckel, 2013). Thus, conodonts from sample Okz-CO-03 indicate the lower Gzhelian.

The lower to middle part of the red siliceous claystone in Okoshizawa (samples Okz-CO-03.1, -03.2 and -04) yielded *St. bellus* and comparable specimens. This is a zonal marker species of the upper Gzhelian around the East European Platform (Chernykh, 2005; Chernykh, 2006; Goreva and Alekseev, 2010) as well as Midcontinent United States (Barrick et al., 2013; Barrick et al., 2022). This species also occurs from the upper Gzhelian of South China (Wang and Qi, 2003). In Okoshizawa, the range of *St. bellus* and comparable specimens parallel the range of *St. elongatus*, which appears in the upper part of the range of *St. bellus* in the Urals (Schmitz and Davydov, 2012), Midcontinent United States (Boardman et al., 2009) and South China (Wang and Qi, 2003). *Streptognathodus elongatus* is also known from the upper Gzhelian in western United States (Ritter, 2020). *Streptognathodus* cf. *flexuosus* and *St. conjunctus* occurred in the lower samples containing *St. bellus* in Okoshizawa. *Streptognathodus flexuosus* occurs in the upper part of the range of *St. bellus* in the Urals (Schmitz and Davydov, 2012) and Midcontinent United States (Boardman et al., 2009) and *St. conjunctus* occurs from the uppermost Gzhelian with *St. elongatus* in the Urals (Barskov et al., 1981; Chernykh and Reshetkova, 1987), Midcontinent United States (Boardman et al., 2009) and western United States (Ritter, 2020). Hence, the lower to middle part of the red siliceous claystone is correlated to the upper Gzhelian.

Sample Okz-CO-04.2 from the upper part of the red siliceous claystone yielded *St. constrictus*. This species characterizes the Asselian in the Urals (Chernykh, 2005, 2006; Chernykh et al., 2020), Novaya Zemlya (Sobolev and Nakrem, 1996), Midcontinent United States (Boardman et al., 2009), Nevada (Beauchamp et al., 2022b) and the Sverdrup Basin (Beauchamp et al., 2022a). Due to its wide distribution, *St. constrictus* has been proposed as a marker species for an international zonation (Henderson, 2018). From the top of the red siliceous claystone in Okoshizawa (sample Okz-CO-043), we obtained *M. belladontae*, *M. dentiseparata* and *M. striata*, the lattermost of

which also occurred higher in the grey bedded chert (sample Okz-CO-04.4). These three species occur from the Asselian in the Urals (Chernykh, 2005; Chernykh, 2006; Chernykh et al., 2020), Novaya Zemlya (Sobolev and Nakrem, 1996), Nevada (Beauchamp et al., 2022b) and the Sverdrup Basin (Beauchamp et al., 2022a), with the LOs of *M. belladontae* and *M. dentiseparata* in the lower Asselian (except for Nevada where the latter appears in the middle Asselian), and the LO of *M. striata* and the highest occurrence of *M. belladontae* in the middle Asselian. The conodonts indicate that the upper part of the red siliceous claystone to the lower part of the grey chert is correlated to the Asselian.

The highest sample in Okoshizawa yielded *M. bisselli*, *M.* cf. *bisselli*, *M.* cf. *intermedia* and *Sw.* cf. *asymmetricus*. The cooccurrence of *M. bisselli*, *M. intermedia* and *Sw. asymmetricus* is recorded in the middle Artinskian of Nevada (Beauchamp et al., 2022b) and the Sverdrup Basin (Beauchamp et al., 2022a). *Mesogondolella intermedia* has not been reported from the Urals, but this absence is interpreted as a result of the disappearance of *Mesogondolella* in the middle Artinskian in the Urals due to shallowing of the depositional environment (Henderson, 2018). The three species also cooccur in Artinskian limestone deposited on Panthalassic seamounts (Igo, 1981; *Sw. asymmetricus* is referred to as *Sweetognathus whitei* therein). Hence, the conodonts from this sample indicate the middle Artinskian.

To summarize the above, the main part of the Okoshizawa section is correlated to the Geologic Time Scale as follows: the green siliceous claystone is correlated to the lower Gzhelian, the lower to middle part of the red siliceous claystone to the upper Gzhelian, the upper part of the red siliceous claystone to the lower to middle Asselian, the lower part of the grey bedded chert to the upper Asselian and the upper part of the grey chert to the middle Artinskian (Figure 4). Kasimovian and Sakmarian strata have not been confirmed by conodonts, which is probably a result of insufficient sampling density in these deep-sea rocks with very low sedimentation rates. Regarding the position of the CPB, *St. isolatus*, which defines the boundary, was not found in the present study. The most important species that constrain the CPB in the Okoshizawa section are *St. bellus* and *St. constrictus*. The former is restricted to the Gzhelian in the Ural region (Chernykh and Ritter, 1997; Schmitz and Davydov, 2012) and Midcontinent United States (Boardman et al., 2009), while it enters the basal Asselian in South China (Wang and Qi, 2003). The latter species occurs above the CPB in the lower Asselian in the Urals (Chernykh, 2005, 2006; Chernykh et al., 2020), Novaya Zemlya (Sobolev and Nakrem, 1996), Midcontinent United States (Boardman et al., 2009), Nevada (Beauchamp et al., 2022b) and the Sverdrup Basin (Beauchamp et al., 2022a). Therefore, we place the CPB between the occurrence of these two species in the Okoshizawa section. Sample Okz-CO-04.1 is positioned within this interval, but unfortunately did not yield conodonts that allow further robust age constraints. A specimen from this sample that offers an additional hint for the placement of the CPB is *St.* aff. *postsigmoidalis*, which has a weakly sigmoidal alignment of the blade, carina and median groove. In the above features it has an affinity with Asselian lineages from *Streptognathodus cristellaris* to *St. postsigmoidalis* or to *Streptognathodus plenus* (Chernykh, 2006). If our specimen belongs to this lineage, the CPB should be placed below this sample, but this argument remains highly speculative at this point.

Two *Streptognathodus* species from Okoshizawa do not show the same stratigraphic distribution as other regions. *Streptognathodus* cf. *elongianus* was found in sample Okz-CO-03.2 with *St. conjunctus* and *St. elongatus*. *Streptognathodus elongianus* was described from the basal part of the range of *St. bellus* in Midcontinent United States, and below the LO of *St. flexuosus* and *St. conjunctus* (Boardman et al., 2009) and is also known from below the LO of the latter two species in New Mexico (Lucas et al., 2017). This species is not reported outside the United States, and its stratigraphic distribution on the global scale may need further consideration. We identified *St. verus* in two samples. This species is known to occur above *St. constrictus* in the Urals (Chernykh, 2005, 2006) and Midcontinent United States (Henderson, 2018), and the occurrence in Okoshizawa is considerably older. Therefore, our specimens may represent a separate species.

5.2 Faunal characteristics

Out of all conodont elements found in the Okoshizawa section, only a minor portion was identified to the species level due to the paucity of well-preserved specimens. This situation generally prohibits discussions about the faunal characteristics of the section at the species level. On the other hand, inferences can be made on faunal characteristics at higher taxonomic levels (e.g., *Streptognathodus* vs. *Mesogondolella*).

As explained above, the basal part of the Okoshizawa section is correlated to the lower Moscovian. In the well-studied sections in the Donets Basin, Bashikirian Mountains, western and central United States and South China, lower Moscovian strata are generically rich, and yield species of *Adetognathus*, *Declinognathodus*, *Diplognathodus*, *Hindeodus*, "*Streptognathodus*" and *Swadelina* in addition to *Idiognathoides*, *Idiognathodus*, *Neognathodus*, *Mesogondolella* and *Gondolella* (Lane and Straka, 1974; Baesemann and Lane, 1985; Nemyrovskaya et al., 1999; Stamm and Wardlaw, 2003; Qi et al., 2014; Qi et al., 2016). Despite the fact that the number of identified conodont elements in the Okoshizawa sample is not so large, we recognized the latter five genera. Although not confirmed in this study, Ehiro et al. (2008) reported *Idiognathodus delicatus*, *Diplognathodus atetsuensis* and *Diplognathodus coloradoensis* from the same interval of the Okoshizawa section. Lower Moscovian seamount limestones of pelagic Panthalassa, also yield diverse conodonts consisting of *Idiognathoides*, *Idiognathodus*, *Neognathodus*, *Mesogondolella*, *Hindeodus* and "*Streptognathodus*" (Koike, 1967; Ishida et al., 2013; Takahashi et al., 2020). Thus, the early Moscovian conodont fauna in pelagic Panthalassa was diverse at the generic level both in shallow and deep areas, and many of the genera known from peri-continental regions were also present in the ocean thousands of kilometres away from the nearest continents. An exception may be *Adetognathus*, which is regarded to be a nearshore taxon (Driese et al., 1984; Davis and Webster, 1985), consistent with the fact that it has not been recovered from Okoshizawa or the seamount limestones.

The most striking feature in the faunal character of the Okoshizawa section is the abrupt change from a *Streptognathodus*-dominated fauna to a *Mesogondolella*-dominated fauna in the Asselian (Figure 4; Supplementary Table S2). Although *Mesogondolella*-like platform elements do occur below this transition, their abundance is inferior compared to *Streptognathodus*. The shift in dominant taxon from *Streptognathodus* to *Mesogondolella* is also suggested in another pelagic deep-sea section in Shizugawa, Kyoto, Southwest Japan, although details on their abundance is not mentioned (Kusunoki et al., 2004). *Mesogondolella* is regarded as a deep-water taxon and their abundance is controlled by fluctuations in sea-levels as well as "actual" origination and extinction (Henderson, 2018; Beauchamp et al., 2022b). For example, the disappearance of this genus in the Artinskian in the Urals is considered as a result of shallowing, while its complete absence in the Midcontinent United States is attributed to the consistently shallow setting (Henderson, 2018). On the other hand, the strata of the Okoshizawa section were deposited on a pelagic deep seafloor that received little or no effect of sea level changes, reflected in the constantly very fine-grained and carbonate-lacking lithology of the main part of the section. Therefore, the sudden faunal change in the Okoshizawa section is unrelated to sea level change and is rather attributed to ecological replacement of *Streptognathodus* by *Mesogondolella* in pelagic Panthalassa, perhaps as a result of competition. *Mesogondolella* appeared in the lower Asselian in the Urals (Chernykh, 2005; Chernykh, 2006; Chernykh et al., 2020), western United States (Wardlaw et al., 2015; Beauchamp et al., 2022b) and the Sverdrup Basin (Beauchamp et al., 2022a), but were not yet abundant in pelagic Panthalassa, where *Streptognathodus* remained dominant. By the middle Asselian, *Mesogondolella* proliferated and spread into pelagic Panthalassa, apparently forcing *Streptognathodus* into demise. Early Cisuralian *Mesogondolella* was long unreported from outside the Urals, but were recently shown to be present in western United States and the Sverdrup Basin (see references above). The result of this study extends the confirmed palaeogeographic domain of *Mesogondolella* and further strengthens the basis for using the taxon for global correlation of the lower Cisuralian. Since the stratigraphic range of *Mesogondolella* species is sometimes difficult to deduce from peri-continental sections due to the effect of sea level changes, pelagic deep-sea sections such as the Okoshizawa section would be important reference sections to elucidate the timing of origination and extinction of these taxa.

The genus *Streptognathodus*, along with *Idiognathodus*, includes species that are found ubiquitously in various environments, while some of its members are thought to have environmentally restricted habitats (Merril and von Bitter, 1984). In particular, Henderson (2018) pointed out that *Streptognathodus* was ecologically replaced by *Sweetognathus*, which is a shallow-water taxon (Petryshen et al., 2020; Beauchamp et al., 2022b). This is seemingly contradictory with the dominance of *Streptognathodus* in the pelagic deep-sea sedimentary rocks in Okoshizawa in the Gzhelian to lower Asselian and its replacement not by *Sweetognathus* but by *Mesogondolella* in the middle Asselian. However, we draw attention to the fact that the youngest members of *Streptognathodus* are known from the upper Asselian in peri-continental regions (Boardman et al., 2009; Chernykh et al., 2020; Beauchamp et al., 2022a, b) and that they have not been recovered in Okoshizawa. We infer that these late Asselian *Streptognathodus* holdovers were generally restricted to shallow seas near landmasses similar to its ecological successor, *Sweetognathus*, as Henderson (2018) stated. On the other hand, *Streptognathodus* of ecological niche in deeper waters were probably driven into extinction by proliferating *Mesogondolella* in the middle Asselian.

The conodont *Streptognathodus isolatus*, which defines the CPB in the GSSP in Aidaralash, Kazakhstan, was not recovered in this study. This is partly contributing to the difficulty in placing the CPB in the Okoshizawa section. The diagnostic feature of *St. isolatus* is the presence of accessory nodes on the caudal lobe of the platform, separated from the platform by a narrow groove. In the Okoshizawa section, we found no *Streptognathodus* with accessory nodes or lobes on the platform. Thus, not only *St. isolatus*, but all *Streptognathodus* species possessing accessory nodes and lobes are absent. This is also the case with the pelagic deep-sea section in Shizugawa, Kyoto (Kusunoki et al., 2004). While the absence of *St. isolatus* may be a result of insufficient sampling density, the total absence of lobed or node-bearing *Streptognathodus* throughout the Okoshizawa section cannot be explained simply by sparsity of sampled horizons. For example, *Streptognathodus wabaunsensis*, a species that bears accessory nodes on the caudal lobe that cooccurs with *St. elongatus* in the upper Gzhelian in both Kazakhstan (Chernykh and Ritter, 1997) and Midcontinent United States (Boardman et al., 2009), was not found in our samples, nor were any *Streptognathodus* with accessory nodes found within the corresponding interval. Although further research on more numerous specimens of this genus is desired, *Streptognathodus* with accessory nodes and lobes seem to be rare or absent in the Gzhelian to middle Asselian pelagic deep areas of Panthalassa and may have been members of this genus that have a somewhat restricted distribution.

Finally, a noteworthy specimen is *Gondolella* sp. in the upper Gzhelian sample. This specimen has a widely inflated, thin-walled and ventrally extended basal cavity and a completely reduced platform showing similarities with the Gzhelian genus *Solkognathus* and the Permian genus *Vjalovognathus* (Figures 5G, 7F). It has been proposed that both *Vjalovognathus* and *Solkognathus* developed from *Gondolella* with reduced or no platforms (Nicoll and Metcalfe, 1998; Yuan et al., 2016). *Solkognathus* is only represented by one species in the upper Gzhelian of the Urals (Chernykh, 2005), while *Vjalovognathus* is a genus restricted to peri-Gondwana seas that appeared in the Sakmarian (Nicoll and Metcalfe, 1998; Mei and Henderson, 2001; Yuan et al., 2016). Similar forms are also reported from Gzhelian or Asselian chert deposited in pelagic deep Panthalassa (Plate 2, Figures 8, 9 in Kusunoki et al., 2004). Present knowledge on this group in the Gzhelian to Asselian interval is limited, but they may have originated in the Ural region and spread elsewhere in the Gzhelian, then became restricted to peri-Gondwanan regions by the Sakmarian.

6 Conclusion

We investigated a siliceous deep-sea section (the Okoshizawa section) in Northeast Japan that was accumulated in pelagic Panthalassa. While some conodont fossils were obtained by conventional dilute HF acid dissolution, a large number of conodonts were observed using a laboratory-based X-ray microscope on specimens found on rock pieces by an optic microscope. The increase in efficiency of observing conodonts from these rocks made it possible to identify enough specimens to make correlations with other regions and make inferences on the faunal characteristics of conodonts in pelagic deep areas of Panthalassa. Based on the obtained conodonts, the section was dated as early Moscovian to middle Artinskian. Important age indicators such as *Id. sinuatus*, *St. vitali*, *St. bellus*, *St. elongatus*, *St. constrictus*, *M. belladontae*, *M. dentiseparata*, *M. striata* and *M. bisselli* were recognized by images obtained by X-ray μCT. The CPB is placed between the occurrences of *St. bellus* and *St. constrictus*. Asselian species of *Mesogondolella* were documented for the first time in pelagic Panthalassa, supporting the validity of these species for global correlation. In the Okoshizawa section, the conodont fauna changes drastically from a *Streptognathodus*-dominated one to a *Mesogondolella*-dominated one in the middle Asselian. This turnover probably reflects an ecological replacement of *Streptognathodus* by *Mesogondolella* in pelagic deep areas of Panthalassa.

Data availability statement

The original contributions presented in the study are included in the article/Supplementary Material, further inquiries can be directed to the corresponding authors.

Author contributions

SM designed the research, carried out the field investigation, sample collection, sample processing, X-ray scans, SEM phtotography and wrote the manuscript. ST took part in initiating the research and manuscript editing. MM collaborated in the initiation of the research, took care of X-ray scanning and edited the manuscript. All authors contributed to the article and approved the submitted version.

Funding

This study was supported by JSPS Grant-in-Aid for Research Activity Start-up Grant Number 19K23470.

Acknowledgments

The authors are deeply indebted to Kazuko Yoshizawa for helping us with finding references and producing illustrations, to Masanori Ozeki for assistance in laboratory work and illustrations, to Shinsuke Yagyu and Takuya Matsuzaki for their support during X-ray scans, to Noritoshi Suzuki for sharing his collection of literature and to Koji Seike for his help in 3D-visualization of conodonts using Amira Software. We are grateful to two reviewers Andrey Zhuravlev and Li Tian and editor Pauline Guenser who helped improve the manuscript. This study was performed under the cooperative research program of Center for Advanced Marine Core Research (CMCR), Kochi University, Accept Nos. 22A048 and 22B043.

Conflict of interest

The authors declare that the research was conducted in the absence of any commercial or financial relationships that could be construed as a potential conflict of interest.

Publisher's note

Supplementary material

The Supplementary Material for this article can be found online at: https://www.frontiersin.org/articles/10.3389/feart.2023.1162023/full#supplementary-material

References

Akhmetshina, L. Z., Barskov, I. S., and Isakova, T. N. (1984). Gzhelian, asselian, and sakmarian conodonts from the Russian platform, southern Urals, and pre-caspian basin. *Trans. Mosc. State Univ.* 13, 51–54. (in Russian).

Baesemann, J. F., and Lane, H. R. (1985). Taxonomy and evolution of the genus Rhachistognathus Dunn (conodonta; late Mississippian to early middle Pennsylvanian). *Cour. Forsohungsinstitut Senckenb.* 74, 93–136.

Barrick, J. E., Alekseev, A. S., Blanco-Ferrera, S., Goreva, N. V., Hu, K., Lambert, L. L., et al. (2022). Carboniferous conodont biostratigraphy. *Geol. Soc. Lond. Spec. Publ.* 512, 695–768. doi:10.1144/sp512-2020-38

Barrick, J. E., Lambert, L. L., Heckel, P. H., and Boardman, D. R. (2004). Pennsylvanian conodont zonation for midcontinent north America. *Rev. Española Micropaleontol.* 36, 231–250.

Barrick, J. E., Lambert, L. L., Heckel, P. H., Rosscoe, S. J., and Boardman, D. R. (2013). Midcontinent Pennsylvanian conodont zonation. *Stratigraphy* 10, 55–72.

Barskov, I. S., Isakova, T. N., and Schastlivcheva, N. P. (1981). Conodonts of the gzelian and asselian boundary beds, southern Urals. *Izvesiya Acad. Nauk. SSR, Seriya Geol.* 5, 78–87. (in Russian).

Beauchamp, B., González, D. C., Henderson, C. M., Baranova, D. V., Wang, H., and Pelletier, E. (2022a). Late pennsylvanian–early permian tectonically driven stratigraphic sequences and carbonate sedimentation along northern margin of Sverdrup Basin (otto fiord depression, arctic Canada). *SEPM Spec. Publ.* 113, 226–254. doi:10.2110/sepmsp.113.12

Beauchamp, B., Henderson, C. M., Dehari, E., Von Bassenheim, D. W., Elliot, S., and González, D. C. (2022b). Carbonate sedimentology and conodont biostratigraphy of late pennsylvanian–early permian stratigraphic sequences, carlin canyon, Nevada: New

insights into the tectonic and oceanographic significance of an iconic succession of the Basin and range. *SEPM Spec. Publ.* 113, 34–71. doi:10.2110/sepmsp.113.14

Boardman, D. R., II, Wardlaw, B. R., and Nestell, M. K. (2009). *Stratigraphy and conodont biostratigraphy of the uppermost carboniferous and lower permian from the North American midcontinent [also on CD]*. Lawrence: Kansas Geological Survey, 42.

Cardoso, C. N., Sanz-López, J., and Blanco-Ferrera, S. (2017). Pennsylvanian conodonts from the tapajós group (amazonas basin, Brazil). *Geobios* 50, 75–95. doi:10.1016/j.geobios.2017.02.004

Chernykh, V. V., Chuvashov, B. I., Shen, S. Z., Henderson, C. M., Yuan, D. X., and Stephenson, M. H. (2020). The global stratotype section and point (GSSP) for the base-sakmarian stage (cisuralian, lower permian). *Episodes* 43, 961–979. doi:10.18814/EPIIUGS/2020/020059

Chernykh, V. V. (2006). Lower permian conodonts in the Urals. *Ekaterinburg Inst. Geol. Geochem. Uralian Branch Russ. Acad. Sci*, 130.

Chernykh, V. V., and Reshetkova, N. P. (1987). The biostratigraphy and conodonts from Carboniferous–Permian boundary deposits on the west slope of the Urals. *Sverdlovsk Uralian Branch, USSR Acad. Sci*, 53.

Chernykh, V. V., and Ritter, S. M. (1997). Streptognathodus (conodonta) succession at the proposed carboniferous–permian boundary stratotype section, Aidaralash Creek, northern Kazakhstan. *J. Paleontol.* 71, 459–474. doi:10.1017/s0022336000039470

Chernykh, V. V. (2005). *Zonal method in biostratigraphy, zonal conodont scale of the Lower Permian in the Urals*. Ekaterinburg: Institute of Geology and Geochemistry of RAN. (in Russian), 217.

Clark, D. L., and Mosher, L. C. (1966). Stratigraphic, geographic, and evolutionary development of the conodont genus Gondolella. *J. Paleontol.* 40, 376–394.

Cnudde, V., and Boone, M. N. (2013). High-resolution X-ray computed tomography in geosciences: A review of the current technology and applications. *Earth-Sci. Rev.* 123, 1–17. doi:10.1016/j.earscirev.2013.04.003

Cunningham, J. A., Rahman, I. A., Lautenschlager, S., Rayfield, E. J., and Donoghue, P. C. J. (2014). A virtual world of paleontology. *Trends Ecol. Evol.* 29, 347–357. doi:10.1016/j.tree.2014.04.004

Davis, L. E., and Webster, G. D. (1985). Late mississippian to early pennsylvanian conodont biofacies in central Montana. *Lethaia* 18, 67–72. doi:10.1111/j.1502-3931.1985.tb00685.x

Davydov, V. I., Barskov, I. S., Bogoslovskaya, M. F., Leven, E. Y., Popov, A. V., Akhmetshina, L. Z., et al. (1994). The carboniferous–permian boundary in stratotype sections of the south Urals and its correlation. *Stratigr. Geol. Correl.* 2, 889–906. doi:10.1080/00206819209465643

Davydov, V. I., Glenister, B. F., Spinosa, C., Ritter, S. M., Chernykh, V. V., Wardlaw, B. R., et al. (1998). Proposal of Aidaralash as global stratotype section and point (GSSP) for base of the permian system. *Episodes* 21, 11–18. doi:10.18814/epiiugs/1998/v21i1/003

Driese, S. G., Carr, T. R., and Clark, D. L. (1984). Quantitative analysis of Pennsylvanian shallow-water conodont biofacies, Utah and Colorado. *Geol. Soc. Am. Mem.* 196, 233–250.

Dunn, D. L. (1970). Middle Carboniferous conodonts from Western United States and phylogeny of the platform group. *J. Paleontol.*, 312–342.

Ehiro, M., Yamakita, S., Takahashi, S., and Suzuki, N. (2008). Jurassic accretionary complexes of the North Kitakami Belt in the akka-kuji area, Northeast Japan. *J. Geol. Soc. Jpn.* 114, 121–139. (in Japanese). doi:10.5575/geosoc.114.s121

Fohrer, B., Nemyrovska, T. I., Samankassou, E., and Ueno, K. (2007). The pennsylvanian (moscovian) izvarino section, Donets Basin, Ukraine: A multidisciplinary study on microfacies, biostratigraphy (conodonts, foraminifers, and ostracodes), and paleoecology. *Mem. (The Paleontol. Soc.* 69, 1–85. doi:10.1666/06-121.1

Geological Survey of Japan, AIST (2020) Seamless digital geological map of Japan 1: 200,000. Geological Survey of Japan, AIST.

Goreva, N. V., and Alekseev, A. S. (2010). Upper carboniferous conodont zones of Russia and their global correlation. *Stratigr. Geol. Correl.* 18, 593–606. doi:10.1134/S086959381006002X

Goudemand, N., Orchard, M. J., Tafforeau, P., Urdy, S., Brühwiler, T., Brayard, A., et al. (2012). Early Triassic conodont clusters from South China: Revision of the architecture of the 15 element apparatuses of the superfamily Gondolelloidea. *Palaeontology* 55, 1021–1034. doi:10.1111/j.1475-4983.2012.01174.x

Goudemand, N., Orchard, M. J., Urdy, S., Bucher, H., and Tafforeau, P. (2011). Synchrotron-aided reconstruction of the conodont feeding apparatus and implications for the mouth of the first vertebrates. *Proc. Natl. Acad. Sci. U. S. A.* 108, 8720–8724. doi:10.1073/pnas.1101754108

Grasby, S. E., Bond, D. P. G., Wignall, P. B., Yin, R., Strachan, L. J., and Takahashi, S. (2021). Transient Permian-Triassic euxinia in the southern Panthalassa deep ocean. *Geology* 49, 889–893. doi:10.1130/G48928.1

Guenser, P., Souquet, L., Dolédec, S., Mazza, M., Rigo, M., and Goudemand, N. (2019). Deciphering the roles of environment and development in the evolution of a Late Triassic assemblage of conodont elements. *Paleobiology* 45, 440–457. doi:10.1017/pab.2019.14

Hayashi, S., Iijima, S., Nakajima, T., Sawaguchi, T., Tanaka, H., and Yoshida, H. (1990). Late paleozoic to mesozoic formations in the southwestern Ashio mountains. *Bull. Gunma Prefect. Mus. Hist.* 11, 1–34. (in japanese with English abstract).

Hayashi, S. (1968). The permian conodonts in chert of the adoyama formation, Ashio mountains, central Japan. *Earth Sci. (Chikyu Kagaku)* 22, 63–77. (in Japanese with English abstract and description).

Heckel, P. H. (2013). Pennsylvanian stratigraphy of northern Midcontinent Shelf and biostratigraphic correlation of cyclothems. *Stratigraphy* 10, 3–39.

Henderson, C. M. (2018). Permian conodont biostratigraphy. *Geol. Soc. Spec. Publ.* 450, 119–142. doi:10.1144/SP450.9

Hori, R. S., Yamakita, S., Ikehara, M., Kodama, K., Aita, Y., Sakai, T., et al. (2011). Early triassic (induan) radiolaria and carbon-isotope ratios of a deep-sea sequence from waiheke island, north island, New Zealand. *Palaeoworld* 20, 166–178. doi:10.1016/j.palwor.2011.02.001

Hu, K., Qi, Y., Qi, W., and Wang, Q. (2020). Carboniferous conodont zonation of China. *Newsletters Stratigr.* 53, 141–190. doi:10.1127/nos/2019/0498

Hu, K. Y., Qi, Y. P., Wang, Q. L., Nemyrovska, T. I., and Chen, J. T. (2017). Early pennsylvanian conodonts from the luokun section of luodian, guizhou, south China. *Palaeoworld* 26, 64–82. doi:10.1016/j.palwor.2015.12.003

Huang, J., Martínez-Pérez, C., Hu, S., Zhang, Q., Zhang, K., Zhou, C., et al. (2019). Apparatus architecture of the conodont Nicoraella kockeli (Gondolelloidea, Prioniodinina) constrains functional interpretations. *Palaeontology* 62, 823–835. doi:10.1111/pala.12429

Igo, H. (1981). Permian conodont biostratigraphy of Japan. *Palaeontol. Soc. Jpn. Spec. Pap.* 24, 1–51.

Ishida, K., Suzuki, S., and Inada, N. (2013). Visean – moscovian conodont biostratigraphy of the ko-yama limestone group, Akiyoshi Belt, SW Japan. *Natral Sci. Res. Univ. Tokushima* 27, 29–52.

Isozaki, Y., Maruyama, S., Aoki, K., Nakama, T., Miyashita, A., and Otoh, S. (2010). Geotectonic subdivision of the Japanese islands revisited: Categorization and definition of elements and boundaries of pacific-type (Miyashiro-type) orogen. *Chigaku Zasshi (Jounal Geogr.* 119, 999–1053. (in Japanese with English abstract). doi:10.5026/jgeography.119.999

Isozaki, Y., Maruyama, S., and Furuoka, F. (1990). Accreted oceanic materials in Japan. *Tectonophysics* 181, 179–205. doi:10.1016/0040-1951(90)90016-2

Isozaki, Y., and Matsuda, T. (1980). Age of the tamba group along the hozugawa "anticline". *West. hills Kyoto, Southwest Jpn. J. Geosci. Osaka City Univ.* 23, 115–134.

Jones, D., Evans, A. R., Siu, K. K. W., Rayfield, E. J., and Donoghue, P. C. J. (2012). The sharpest tools in the box? Quantitative analysis of conodont element functional morphology. *Proc. R. Soc. B Biol. Sci.* 279, 2849–2854. doi:10.1098/rspb.2012.0147

Ketcham, R. A., and Carlson, W. D. (2001). Acquisition, optimization and interpretation of X-ray computed tomographic imagery: Applications to the geosciences. *Comput. Geosci.* 27, 381–400. doi:10.1016/S0098-3004(00)00116-3

Koike, T. (1967). A Carboniferous succession of conodont faunas from the Atetsu Limestone in southwest Japan (Studies of Asiatic conodonts, Part 4). *Tokyo Kyoiku Daigaku Sci. Rep. Sect. C Geol. Mineral. Geogr.* 92, 279–318.

Kusunoki, T., Ohara, M., and Musashino, M. (2004). Carboniferous-Permian microbiostratigraphy in chert sequence from the southeastern part of the Tamba Belt, Shizugawa district, Uji City (Outline note). *Earth Sci. (Chikyu Kagaku)* 58, 37–54. (in Japanese with English abstract).

Lane, H. R., and Straka, J. J. (1974). *Late Mississippian and early pennsylvanian conodonts, Arkansas and Oklahoma*. Boulder: Geological Society of America.

Lucas, S. G., Krainer, K., Barrick, J. E., Vachard, D., and Ritter, S. M. (2017). Lithostratigraphy and microfossil biostratigraphy of the pennsylvanian-lower permian horquilla formation at new well peak, big HatchetMountains, new Mexico, USA. *Stratigraphy* 14, 223–246. doi:10.29041/strat.14.1-4.223-246

Martínez-Pérez, C., Rayfield, E. J., Botella, H., and Donoghue, P. C. J. (2016). Translating taxonomy into the evolution of conodont feeding ecology. *Geology* 44, 247–250. doi:10.1130/G37547.1

Matsuda, T., and Isozaki, Y. (1991). Well-documented travel history of Mesozoic pelagic chert in Japan: From remote ocean to subduction zone. *Tectonics* 10, 475–499. doi:10.1029/90tc02134

Mazza, M., and Martínez-Pérez, C. (2015). Unravelling conodont (Conodonta) ontogenetic processes in the Late Triassic through growth series reconstructions and X-ray microtomography. *Boll. della Soc. Paleontol. Ital.* 54, 161–186. doi:10.4435/BSPI.2015.10

Mees, F., Swennen, R., Van Geet, M., and Jacobs, P. (2003). Applications of X-ray computed tomography in the geosciences. *Geol. Soc. London, Spec. Publ.* 215, 1–6.

Mei, S., and Henderson, C. M. (2001). Evolution of Permian conodont provincialism and its significance in global correlation and paleoclimate implication. *Palaeogeogr. Palaeoclimatol. Palaeoecol.* 170, 237–260. doi:10.1016/S0031-0182(01)00258-9

Merrill, G. K., and King, C. W. (1971). Platform conodonts from the lowest Pennsylvanian rocks of northwestern Illinois. *J. Paleontol.*, 645–664.

Merrill, G. K. (1973). Pennsylvanian nonplatform conodont genera I: Spathognathodus. *J. Paleontol.* 47, 289–314.

Merrill, G. K., and von Bitter, P. H. (1984). Facies frequencies among Pennsylvanian conodonts: Apparatuses and abundances. *Geol. Soc. Am. Spec. Pap.* 196, 251–261.

Muto, S., and Ito, T. (2021). Conodont fossils from the kiryu and ashikaga district (quadrangle series 1:50,000), central Japan with emphasis on the reexamination of "Carboniferous" conodonts from the Ashio Belt. *Bull. Geol. Surv. Jpn.* 72, 325–344. doi:10.9795/bullgsj.72.325

Muto, S., Ito, T., and Murayama, M. (2023). Geology and accretionary age of the Otori unit, North Kitakami Belt. *Bull. Geol. Surv. Jpn.* 74, 1–40. doi:10.9795/bullgsj.74.1_1

Muto, S. (2021). Recurrent deposition of organic-rich sediments in Early Triassic pelagic Panthalassa and its relationship with global oceanic anoxia: New data from Kyoto, Southwest Japan. *Glob. Planet. Change* 197, 103402. doi:10.1016/j.gloplacha.2020.103402

Muto, S., Takahashi, S., Yamakita, S., and Onoue, T. (2020). Scarcity of chert in upper Lower Triassic Panthalassic deep-sea successions of Japan records elevated clastic inputs rather than depressed biogenic silica burial flux following the end-Permian extinction. *Glob. Planet. Change* 195, 103330. doi:10.1016/j.gloplacha.2020.103330

Muto, S., Takahashi, S., Yamakita, S., Soda, K., and Onoue, T. (2019). Conodont-based age calibration of the Middle Triassic Anisian radiolarian biozones in pelagic deep-sea bedded chert. *Bull. Geol. Surv. Jpn.* 70, 43–89. doi:10.9795/bullgsj.70.43

Muto, S., Takahashi, S., Yamakita, S., Suzuki, N., Suzuki, N., and Aita, Y. (2018). High sediment input and possible oceanic anoxia in the pelagic Panthalassa during the latest Olenekian and early Anisian: Insights from a new deep-sea section in Ogama, Tochigi, Japan. *Palaeogeogr. Palaeoclimatol. Palaeoecol.* 490, 687–707. doi:10.1016/j.palaeo.2017.11.060

Muto, S., Yagyu, S., Takahashi, S., and Murayama, M. (2021). Identification of conodont fossils in pelagic deep-sea siliceous sedimentary rocks using laboratory-based X-ray computed microtomography. *Lethaia* 54, 687–699. doi:10.1111/let.12432

Nakada, R., Ogawa, K., Suzuki, N., Takahashi, S., and Takahashi, Y. (2014). Late Triassic compositional changes of aeolian dusts in the pelagic Panthalassa: Response to the continental climatic change. *Palaeogeogr. Palaeoclimatol. Palaeoecol.* 393, 61–75. doi:10.1016/j.palaeo.2013.10.014

Nascimento, S., Scomazzon, A., Moutinho, L., Lemos, V., and Matsuda, N. (2005). Conodont biostratigraphy of the lower itaituba formation (atokan, penssylvanian), amazonas basin, Brazil. *Rev. Bras. Paleontol.* 8, 193–202.

Nemirovskaya, T., and Alekseev, A. S. (1994). The bashkirian conodonts of the askyn section bashkirian mountains, Russia. *Bull. Société Belge. Géologie* 103, 109–133.

Nemyrovska, T. I. (1999). Bashkirian conodonts of the Donets Basin, Ukraine. *Scr. Geol.* 25, 1–115.

Nemyrovska, T. I. (2017). Late mississippian-middle pennsylvanian conodont zonation of Ukraine. *Stratigraphy* 14, 299–318. doi:10.29041/strat.14.1-4.299-318

Nemyrovska, T. I. (2011). Late moscovian (carboniferous) conodonts of the genus Swadelina from the Donets Basin, Ukraine. *Micropaleontology* 57, 491–505. doi:10.47894/mpal.57.6.03

Nemyrovska, T. I., Perret-Mirouse, M.-F., and Alekseev, A. S. (1999). On moscovian (late carboniferous) conodonts of the Donets Basin, Ukraine. *Neues Jahrb. Geol. Palaontol. Abh.* 214, 169–194. doi:10.1127/njgpa/214/1999/169

Nemyrovska, T. I., Wagner, R. H., Winkler Prins, C. F., and Montañez, I. (2011). Conodont faunas across the mid-carboniferous boundary from the barcaliente formation at la lastra (Palentian Zone, Cantabrian mountains, Northwest Spain); geological setting, sedimentological characters and faunal descriptions. *Scr. Geol.*, 127–175.

Nicoll, R. S., and Metcalfe, I. (1998). Early and middle permian conodonts from the canning and southern carnarvon basins, western Australia: Their implications for regional biogeography and palaeoclimatology. *Proc. R. Soc. Victoriaety Vic.* 110, 419–461.

Nishikane, Y., Kaiho, K., Takahashi, S., Henderson, C. M., Suzuki, N., and Kanno, M. (2011). The Guadalupian-Lopingian boundary (Permian) in a pelagic sequence from Panthalassa recognized by integrated conodont and radiolarian biostratigraphy. *Mar. Micropaleontol.* 78, 84–95. doi:10.1016/j.marmicro.2010.10.002

Perlmutter, B. (1975). Conodonts from the uppermost wabaunsse group (pennsylvanian) and the admire and council grove groups (permian) in Kansas. *Geol. Palaeontol.* 9, 95–115.

Petryshen, W., Henderson, C. M., De Baets, K., and Jarochowska, E. (2020). Evidence of parallel evolution in the dental elements of Sweetognathus conodonts: Sweetognathus Evolutionary Mechanisms. *Proc. R. Soc. B Biol. Sci.* 287, 20201922. doi:10.1098/rspb.2020.1922

Qi, Y., Hu, K., Wang, Q., and Lin, W. (2014). Carboniferous conodont biostratigraphy of the dianzishang section, Zhenning, Guizhou, South China. *Geol. Mag.* 151, 311–327. doi:10.1017/S0016756813000344

Qi, Y. P., Lambert, L. L., Nemyrovska, T. I., Wang, X. D., Hu, K. Y., and Wang, Q. L. (2016). Late bashkirian and early moscovian conodonts from the naqing section, luodian, guizhou, south China. *Palaeoworld* 25, 170–187. doi:10.1016/j.palwor.2015.02.005

Ritter, S. M. (2020). Improved conodont biostratigraphic constraint of the Carboniferous/Permian boundary in south-central New Mexico, USA. *Stratigraphy* 17, 39–56. doi:10.29041/strat.17.1.39-56

Ritter, S. M. (1995). Upper Missourian–Lower Wolfcampian (Upper Kasimovian–Lower Asselian) conodont biostratigraphy of the midcontinent, U.S.A. *U.S.A. J. Paleontol.* 69, 1139–1154. doi:10.1017/S0022336000038129

Sano, H., Kuwahara, K., Yao, A., and Agematsu, S. (2010). Panthalassan Seamount-Associated Permian-Triassic Boundary Siliceous Rocks, Mino Terrane, Central Japan. *Paleontol. Res.* 14, 293–314. doi:10.2517/1342-8144-14.4.293

Sano, H., Kuwahara, K., yao, A., and Agematsu, S. (2012). Stratigraphy and Age of the Permian-Triassic Boundary Siliceous Rocks of the Mino Terrane in the Mt. Funabuseyama Area, Central Japan. *Paleontol. Res.* 16, 124–145. doi:10.2517/1342-8144-16.2.124

Savage, N. M., and Barkeley, S. J. (1985). Early to middle Pennsylvanian conodonts from the Klawak Formation and the Ladrones Limestone, southeastern Alaska. *J. Paleontol.* 59, 1451–1475.

Schmitz, M. D., and Davydov, V. I. (2012). Quantitative radiometric and biostratigraphic calibration of the Pennsylvanian-Early Permian (Cisuralian) time scale and pan-Euramerican chronostratigraphic correlation. *Bull. Geol. Soc. Am.* 124, 549–577. doi:10.1130/B30385.1

Sobolev, N. N., and Nakrem, H. A. (1996). Middle Carboniferous-Lower Permian conodonts of Novaya Zemlya. *Nor. Polarinst. Skr.* 199, 1–129.

Stamm, R. G., and Wardlaw, B. R. (2003). *Conodont faunas of the late middle pennsylvanian*. USA: Desmoinesian) lower Kittanning cyclothem, 95–121.

Suárez-Riglos, M., Hünicken, M. A., and Merino-Redo, D. A. (1987). "Conodont biostratigraphy of the Upper Carboniferous-Lower Permian rocks of Bolivia," in *Conodont-Investigative techniques and applications-*. Editor R. L. Austin (Chichester: Ellis Horwood Ltd), 317–325.

Sugimoto, M. (1974). Stratigraphical Study in the Outer Belt of the Kitakami Massif, Northeast Japan. *Tohoku Univ. Inst. Geol. Paleontol. Contrib.* 74, 1–60. (in Japanese with English abstract).

Sun, Z.-Y., Liu, S., Ji, C., Jiang, D.-Y., and Zhou, M. (2020). Gondolelloid multielement conodont apparatus (Scythogondolella) from the Lower Triassic of Jiangsu, East China, revealed by high-resolution X-ray microtomography. *Palaeoworld* 30, 286–295. doi:10.1016/j.palwor.2020.06.001

Suzuki, N., Yamakita, S., Takahashi, S., and Ehiro, M. (2007). Middle Jurassic radiolarians from carbonate manganese nodules in the Otori Formation in the eastern part of the Kuzumaki-Kamaishi Subbelt, the North Kitakami Belt, Northeast Japan. *J. Geol. Soc. Jpn.* 113, 274–277. (in japanese with English abstract). doi:10.5575/geosoc.113.274

Takahashi, S., Ehiro, M., Suzuki, N., and Yamakita, S. (2016). Subdivisional scheme of the North Kitakami Belt, Northeast Japan and its tectonostratigraphic correlation to the Oshima and South Chichibu belts: an examination of the Jurassic accretionary complex in the west Akka area. *J. Geol. Soc. Jpn.* 122, 1–22. (in japanese with English abstract). doi:10.5575/geosoc.2015.0034

Takahashi, S., Hori, R. S., Yamakita, S., Aita, Y., Takemura, A., Ikehara, M., et al. (2021). Progressive development of ocean anoxia in the end-Permian pelagic Panthalassa. *Glob. Planet. Change* 207, 103650. doi:10.1016/j.gloplacha.2021.103650

Takahashi, S., Yamakita, S., Suzuki, N., Kaiho, K., and Ehiro, M. (2009). High organic carbon content and a decrease in radiolarians at the end of the Permian in a newly discovered continuous pelagic section: A coincidence? *Palaeogeogr. Palaeoclimatol. Palaeoecol.* 271, 1–12. doi:10.1016/j.palaeo.2008.08.016

Takahashi, S., Yamasaki, S. ichi, Ogawa, Y., Kimura, K., Kaiho, K., Yoshida, T., et al. (2014). Bioessential element-depleted ocean following the euxinic maximum of the end-Permian mass extinction. *Earth Planet. Sci. Lett.* 393, 94–104. doi:10.1016/j.epsl.2014.02.041

Takahashi, Y., Agematsu, S., and Sashida, K. (2020). Bashkirian–Moscovian (Pennsylvanian) conodonts from the pelagic atoll carbonate of the Omi Limestone, Akiyoshi Terrane, central Japan. *Micropaleontology* 66, 351–367. doi:10.47894/mpal.66.4.06

Tomimatsu, Y., Nozaki, T., Sato, H., Takaya, Y., Kimura, J.-I., Chang, Q., et al. (2020). Marine osmium isotope record during the Carnian "pluvial episode" (Late Triassic) in the pelagic Panthalassa Ocean. *Glob. Planet. Change* 197, 103387. doi:10.1016/j.gloplacha.2020.103387

Uchino, T., and Suzuki, N. (2020). Late Jurassic radiolarians from mudstone near the U–Pb-dated sandstone of the North Kitakami Belt in the northeastern Shimokita Peninsula, Tohoku, Japan. *Bull. Geol. Surv. Jpn.* 71, 313–330. doi:10.9795/bullgsj.71.313

von Bitter, P. H. (1972). Environmental control of conodont distribution in the Shawnee Group (Upper Pennsylvanian) of eastern Kansas. *Univ. Kans. Paleontol. Contrib.* 59, 1–105.

von Bitter, P. H., and Merrill, G. K. (1980). *Naked species of* Gondolella *(Conodontophorida): Their distribution, taxonomy, and evolutionary significance*. Germany: Royal Onta. Royal Ontario Museum.

Wakita, K., and Metcalfe, I. (2005). Ocean plate stratigraphy in East and Southeast Asia. *J. Asian Earth Sci.* 24, 679–702. doi:10.1016/j.jseaes.2004.04.004

Wang, Z., and Qi, Y. (2003). Upper Carboniferous (Pennsylvanian) conodonts from South Guizhou of China. *Riv. Ital. Paleontol. Strat.* 109, 379–397.

Wardlaw, B. R., Gallegos, D. M., Chernykh, V. V., and Snyder, W. S. (2015). Early Permian conodont fauna and stratigraphy of the Garden Valley Formation, Eureka County, Nevada. *Micropaleontology* 61, 369–387. doi:10.47894/mpal.61.4.07

Yamakita, S., Kadota, N., Kato, T., Tada, R., Ogihara, S., Tajika, E., et al. (1999). Confirmation of the Permian/Triassic boundary in deep-sea sedimentary rocks; earliest Triassic condonts from black carbonaceous claystone of the Ubara section in the Tamba Belt, Southwest Japan. *J. Geol. Soc. Jpn.* 105, 895–898. doi:10.5575/geosoc.105.895

Yamakita, S., Takemura, A., Kamata, Y., Aita, Y., Hori, S. R., and Campbell, H. J. (2007). A conodont biostratigraphic framework of a Permian/Triassic ocean-floor sequence in the accretionary Waipapa Terrane at Arrow Rocks, Northland, New Zealand. *GNS Sci. Monogr.* 24, 69–85.

Yamashita, D., Kato, H., Onoue, T., and Suzuki, N. (2018). Integrated Upper Triassic Conodont and Radiolarian Biostratigraphies of the Panthalassa Ocean. *Paleontol. Res.* 22, 167–197. doi:10.2517/2017pr020

Yao, A., Matsuda, T., and Isozaki, Y. (1980). Triassic and Jurassic radiolarians from the Inuyama area, central Japan. *J. Geosci. Osaka City Univ.* 23, 135–154.

Yuan, D. X., Zhang, Y. C., Shen, S. Z., Henderson, C. M., Zhang, Y. J., Zhu, T. X., et al. (2016). Early Permian conodonts from the Xainza area, central Lhasa Block, Tibet, and their palaeobiogeographical and palaeoclimatic implications. *J. Syst. Palaeontol.* 14, 365–383. doi:10.1080/14772019.2015.1052027

Zhuravlev, A. V., and Gerasimova, A. I. (2016). XMT micropalaeontological study of the silicites. *Vestn. Inst. Geol. Komi Sci. Cent. Ural. Branch Ras.* 3, 26–32. doi:10.19110/2221-1381-2016-3-26-32

Zhuravlev, A. V. (2017). Histological application of X-ray computed microtomography of conodonts. *Vestn. Inst. Geol. Komi Sci. Cent. Ural. Branch Ras.* 2, 41–44. doi:10.19110/2221-1381-2017-2-41-44

Ziegler, A. M., Hulver, M. L., and Rowley, D. B. (1997). "Permian world topography and climate," in *Late glacial and postglacial environmental changes-quaternary, carboniferous±Permian and proterozoic*. Editor I. P. Martini (New York: Oxford University Press), 111–146.